# LARGE-SCALE MAGNETIC FIELDS OF THE SUN ACCORDING TO OBSERVATIONS IN THE BAIKAL AND SAYAN SOLAR OBSERVATORIES

**M.L.Demidov, R.V.Pavlova, V.S.Peshcherov**

email: demid@iszf.irk.ru

**«Advances in Astronomy and Geophysics»**

**International Conference on the 120th Anniversary**

**of the Bulnay Earthquake**

**Ulaanbaatar, IAG MAS**

**11.08.2025**

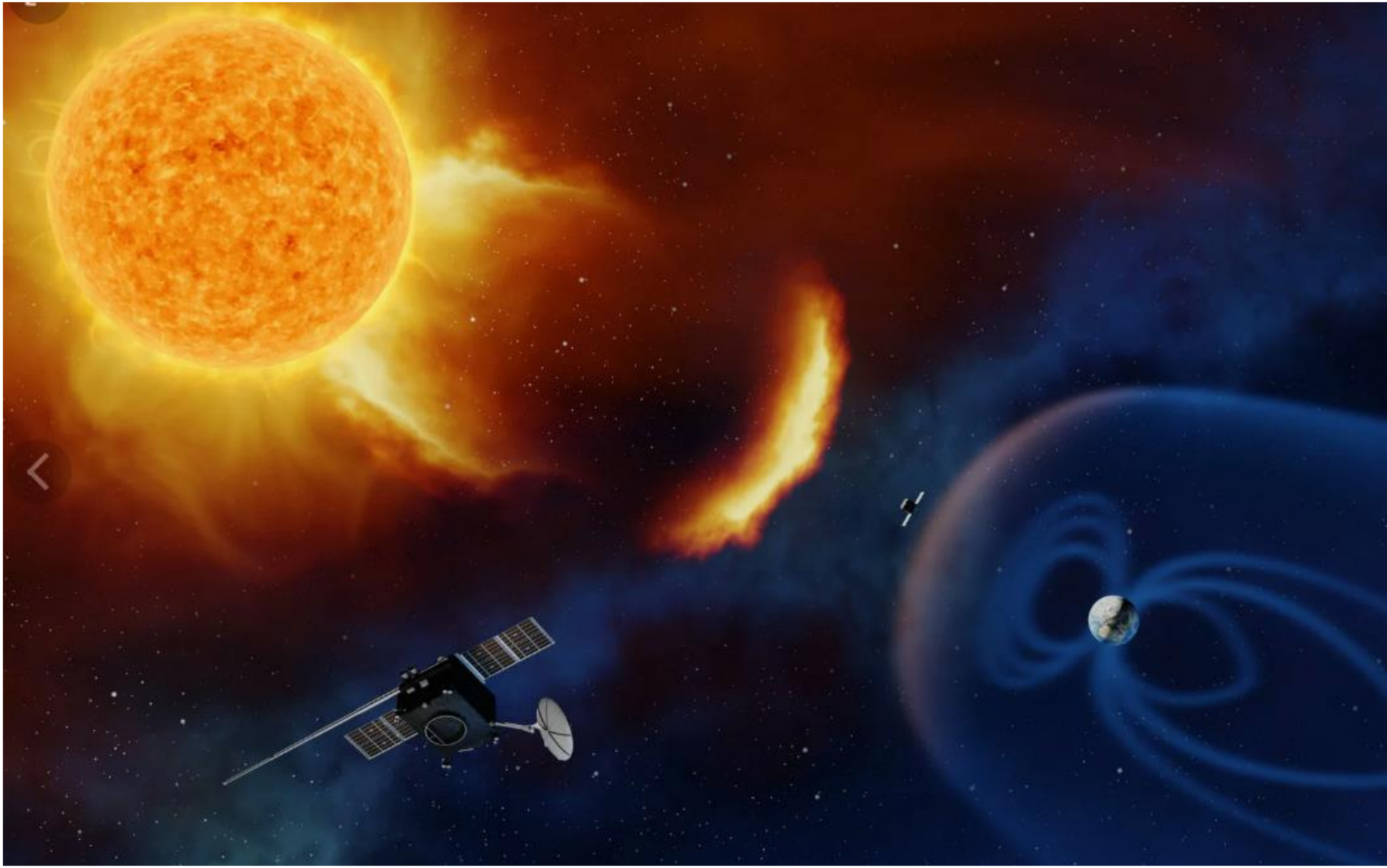

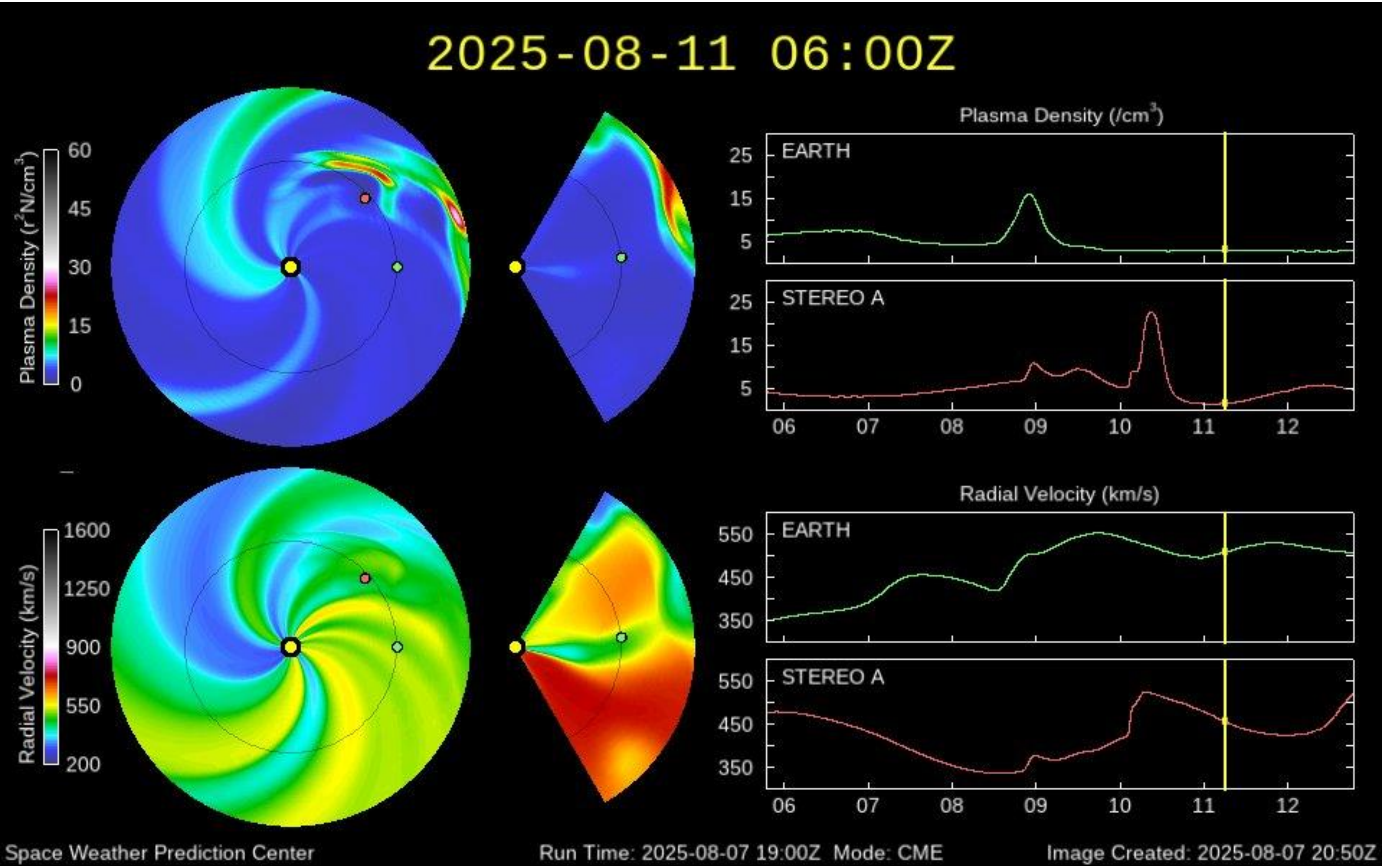
2025-08-11 06:00Z
Plasma Density (r²N/cm³)
60
45
30
15
0
Plasma Density (/cm³)
EARTH
STEREO A
25
15
5
06
07
08
09
10
11
12
Radial Velocity (km/s)
1600
1250
900
550
200
Radial Velocity (km/s)
EARTH
STEREO A
550
450
350
Space Weather Prediction Center
Run Time: 2025-08-07 19:00Z Mode: CME
Image Created: 2025-08-07 20:50Z

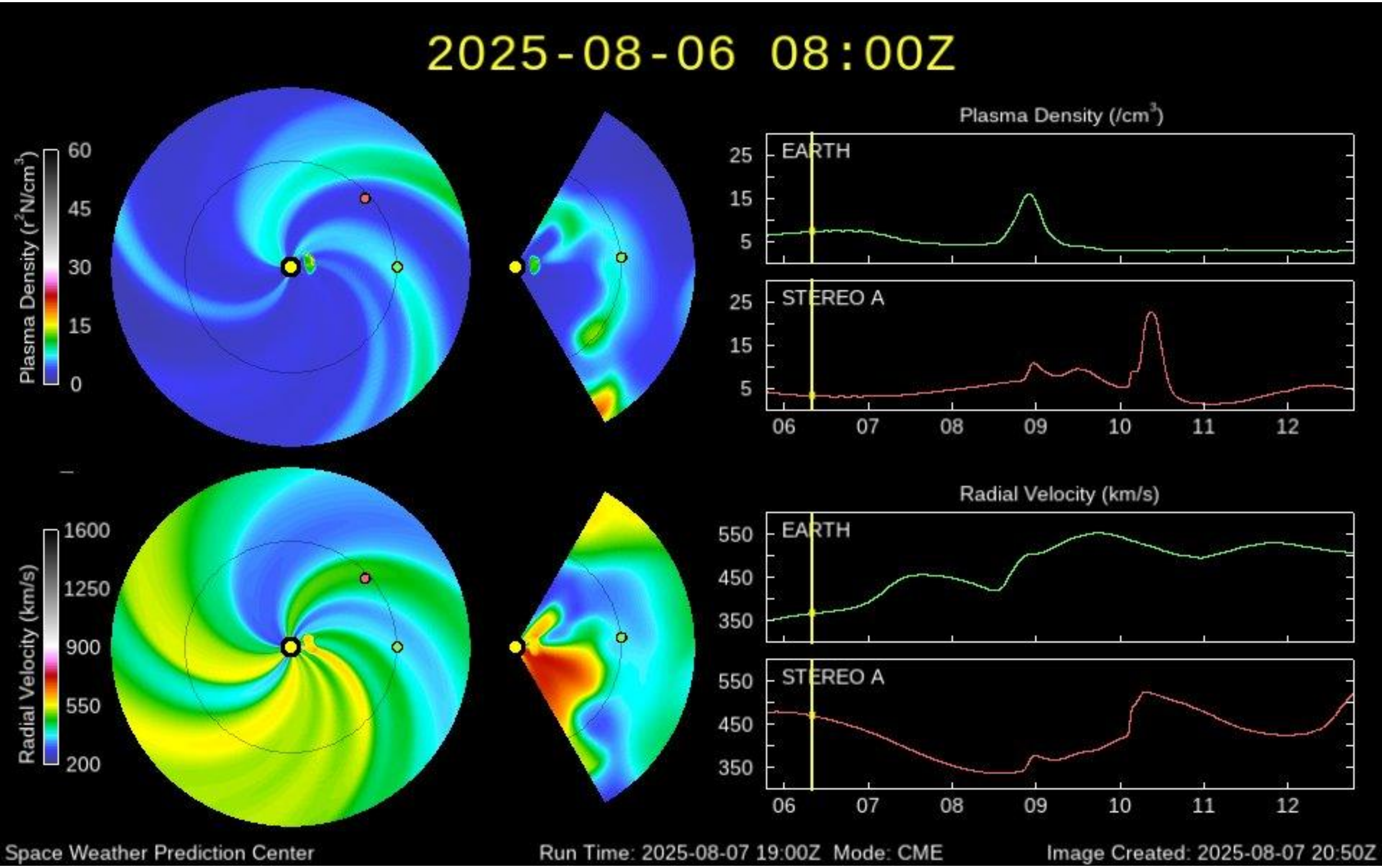

2025-08-06 08:00Z
Plasma Density (r²N/cm³)
60
45
30
15
0
Radial Velocity (km/s)
1600
1250
900
550
200
Plasma Density (/cm³)
EARTH
STEREO A
25
15
5
06
07
08
09
10
11
12
Radial Velocity (km/s)
550
450
350
Space Weather Prediction Center
Run Time: 2025-08-07 19:00Z Mode: CME
Image Created: 2025-08-07 20:50Z

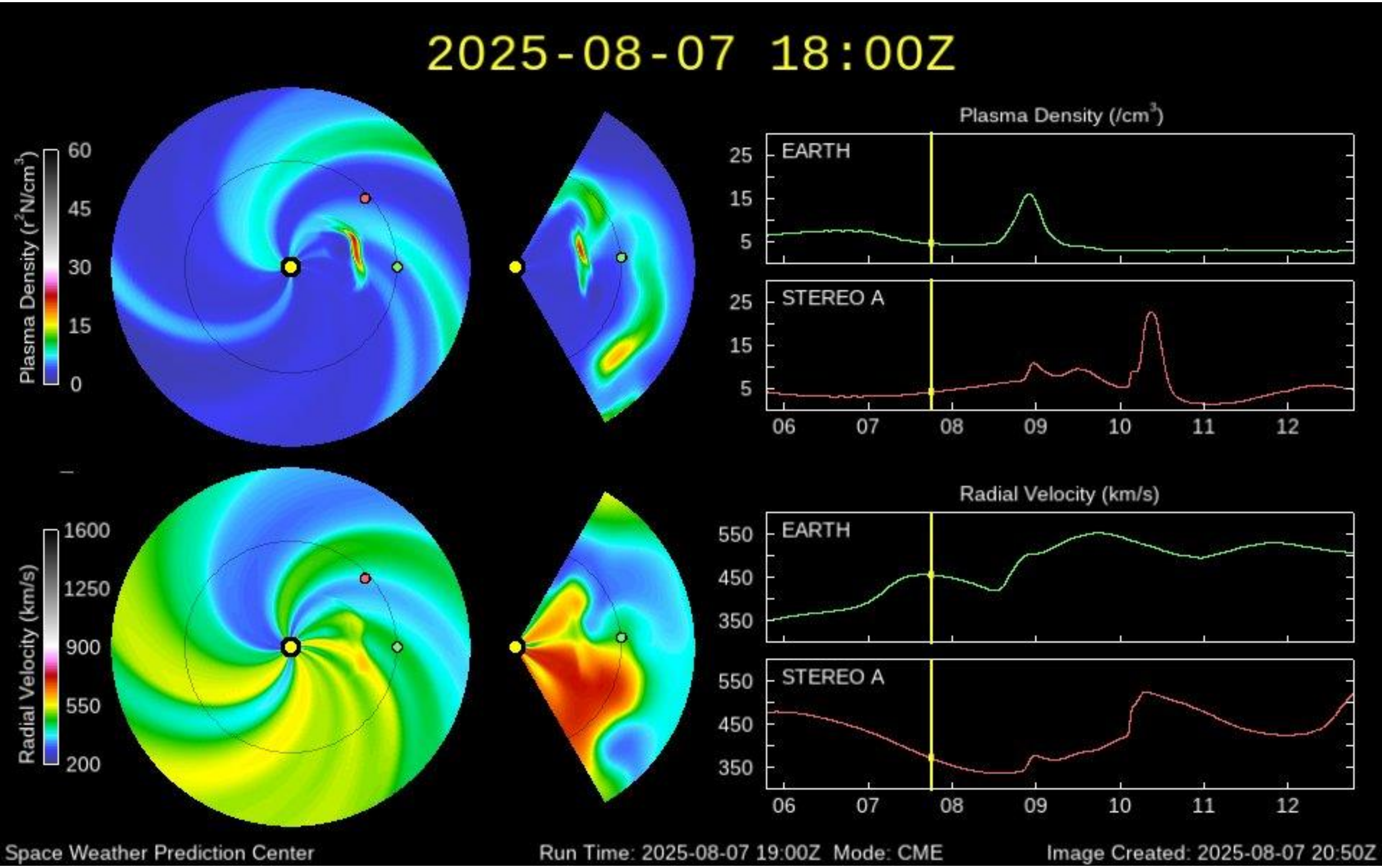

2025-08-07 18:00Z
Plasma Density (r²N/cm³)
60
45
30
15
0
Radial Velocity (km/s)
1600
1250
900
550
200
Plasma Density (/cm³)
EARTH
STEREO A
25
15
5
Radial Velocity (km/s)
550
450
350
06
07
08
09
10
11
12
Space Weather Prediction Center
Run Time: 2025-08-07 19:00Z Mode: CME
Image Created: 2025-08-07 20:50Z

# Geomagnetic Storm WATCHES Aug 08-09

**G1** **G2**

Updated
Aug 06, 2025
1245 MT

WHAT: Combined CME and CH HSS will likely reach Earth and lead to increased geomagnetic activity

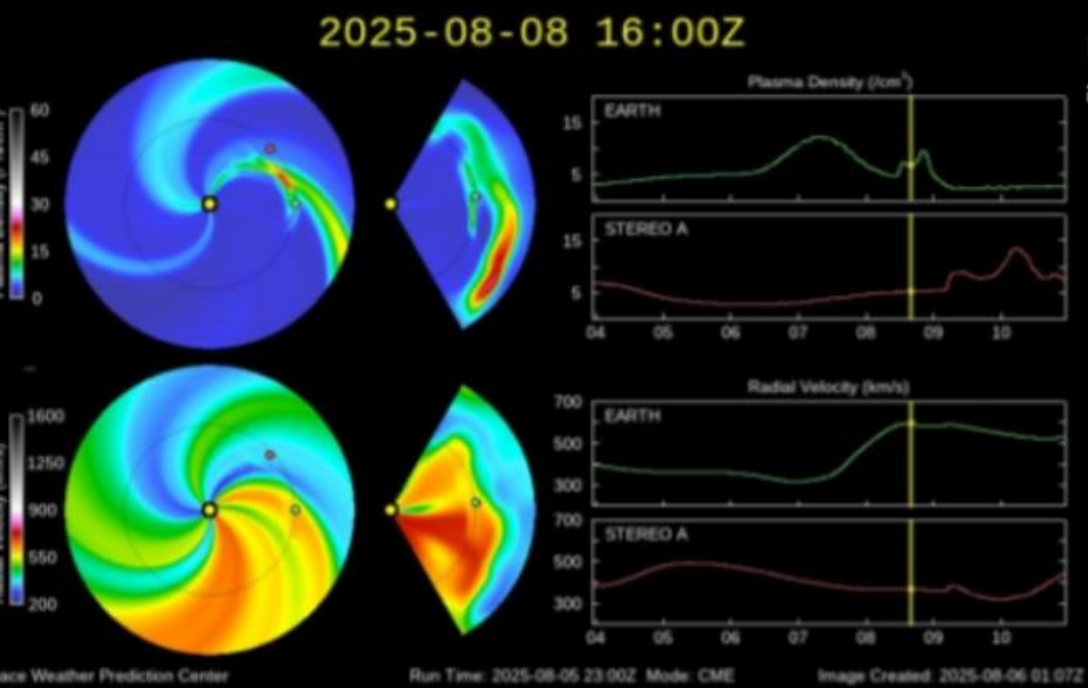


## EVENT:

A coronal mass ejection (CME) is an eruption of lar material and magnetic fields. When they arrive at Earth, a geomagnetic storm can result. Watches of this level are not uncommon.

## EXPECTATION:

A CME and Coronal Hole High Speed Stream (CH HSS) are anticipated to affect Earth with elevated geomagnetic response and dependent upon the orientation of the embedded magnetic field, potential exists for Moderate Storm levels.

## EFFECTS:

Minor - mainly manageable effects to some technological infrastructure. The aurora may become visible over some northern and upper Midwest states from New York to Idaho. Those wishing to see the aurora should visit our webpage for updates.

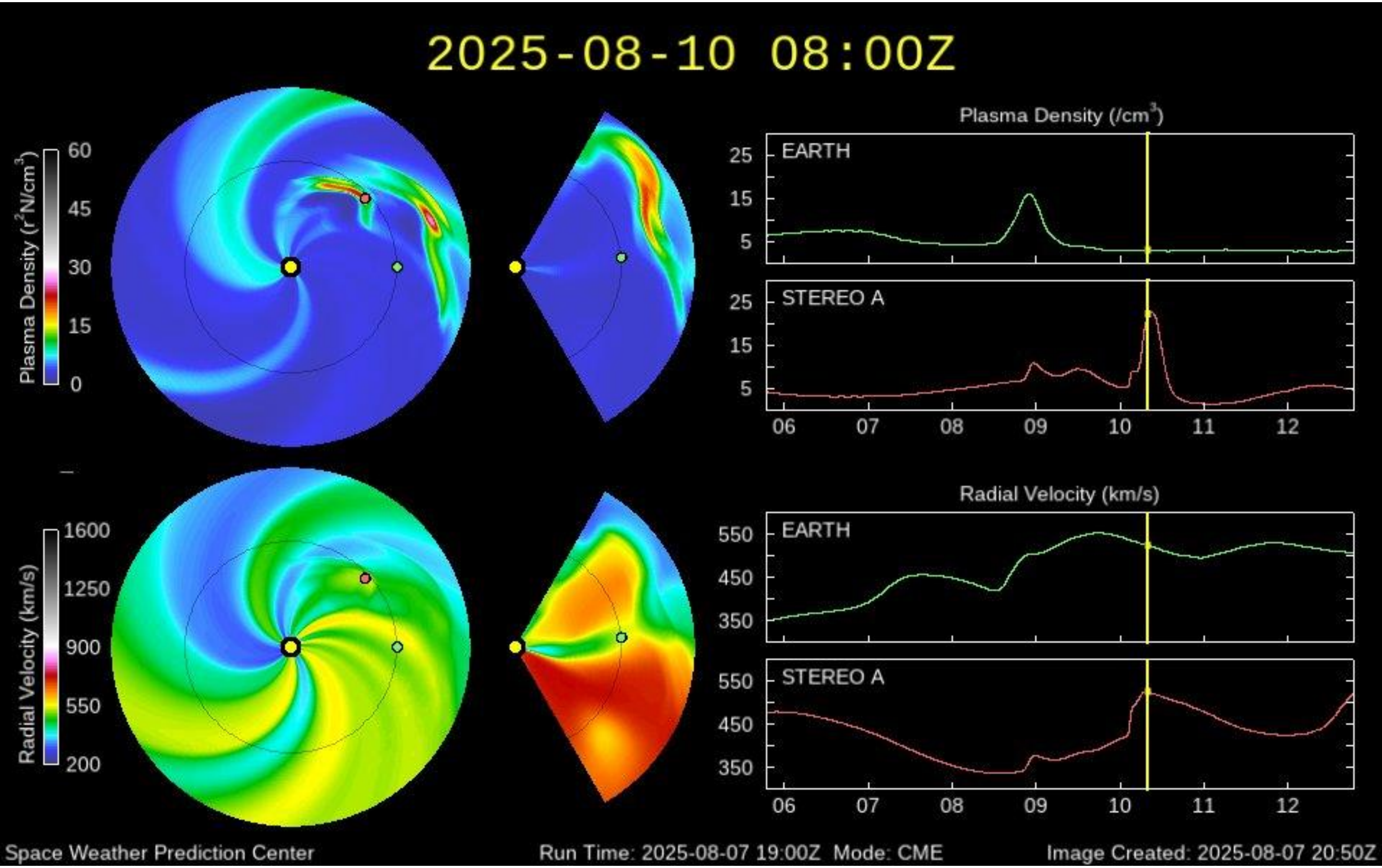

2025-08-10 08:00Z
Plasma Density (r²N/cm³)
60
45
30
15
0
Plasma Density (/cm³)
EARTH
STEREO A
25
15
5
06
07
08
09
10
11
12
Radial Velocity (km/s)
1600
1250
900
550
200
Radial Velocity (km/s)
EARTH
STEREO A
550
450
350
Space Weather Prediction Center
Run Time: 2025-08-07 19:00Z Mode: CME
Image Created: 2025-08-07 20:50Z

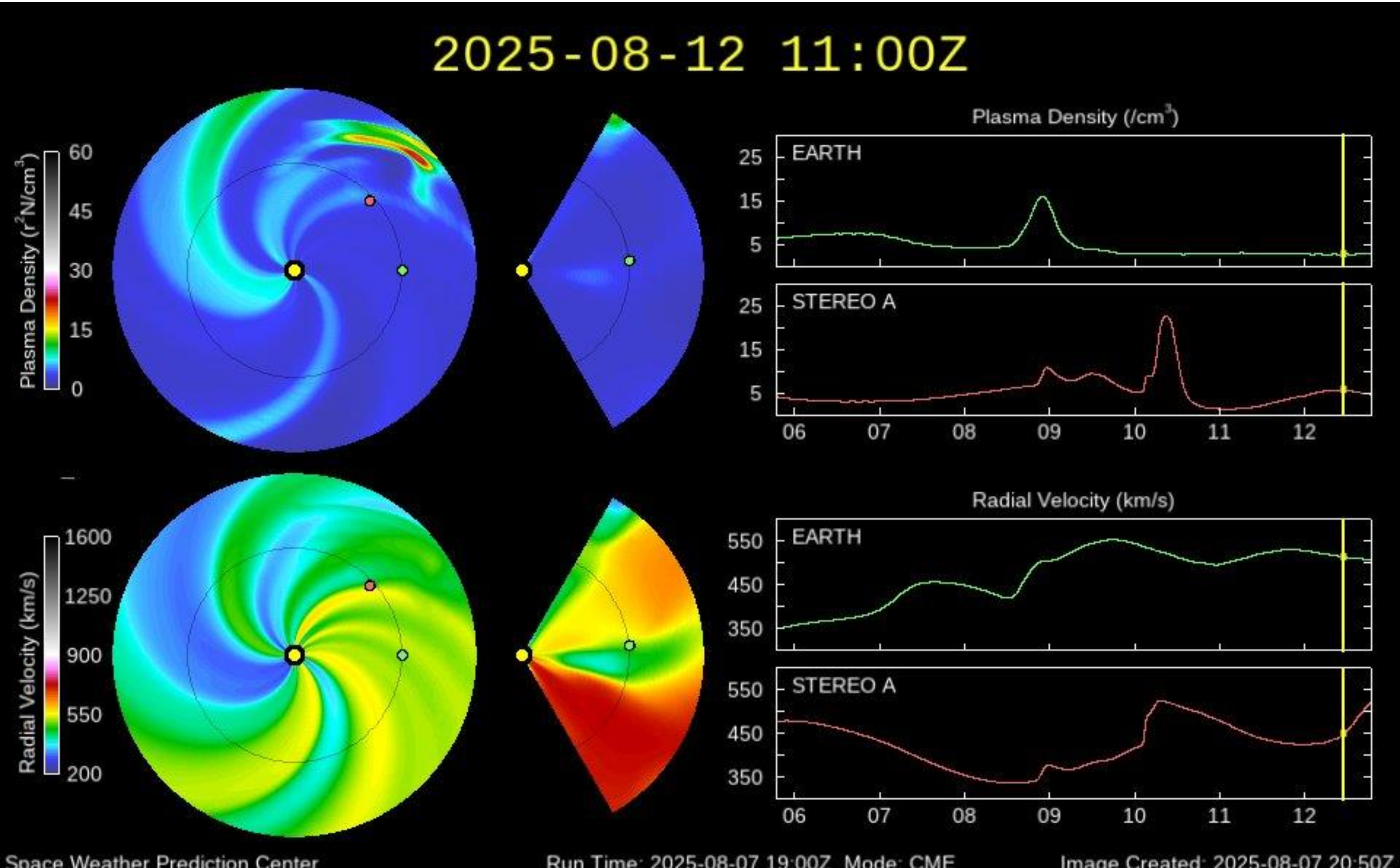

2025-08-12 11:00Z
Plasma Density (r²N/cm³)
60
45
30
15
0
Radial Velocity (km/s)
1600
1250
900
550
200
Plasma Density (/cm³)
EARTH
STEREO A
25
15
5
Radial Velocity (km/s)
550
450
350
06
07
08
09
10
11
12
Space Weather Prediction Center
Run Time: 2025-08-07 19:00Z Mode: CME
Image Created: 2025-08-07 20:50Z

Draft version June 12, 2025
Typeset using LaTeX default style in AASTeX631



# What Causes Errors in Wang-Sheeley-Arge Solar Wind Modeling at L1 ?

Satabdwa Majumdar,[1] Martin A. Reiss,[2] Karin Muglach,[3,4] and Charles N. Arge[3]

[1] Austrian Space Weather Office, GeoSphere Austria, Graz, 8020, Austria
[2] Community Coordinated Modeling Center, NASA Goddard Space Flight Center, 8800 Greenbelt Rd., Greenbelt, MD 20771, USA
[3] NASA Goddard Space Flight Center, 8800 Greenbelt Rd., Greenbelt, MD 20771, USA
[4] Catholic University of America, Washington, DC 20064, USA

## ABSTRACT

Previous ambient solar wind (SW) validation studies have reported on discrepancies between modeled and observed SW conditions at L1. They indicated that a major source of discrepancies stems from how we model the solar corona. Thus, enhancing predictive capabilities demands a thorough examination of coronal modeling. The Wang-Sheeley-Arge (WSA) model has been a workhorse model that provides the near-Sun SW conditions. An important component of it is the Potential Field Source Surface (PFSS) model. This study analyzes 15 different Carrington Rotations (CRs), and presents detailed analysis of CR 2052 to identify WSA model settings that lead to successful and erroneous SW predictions at Earth. For the events studied, we show that increasing the model's grid resolution improves the open-close boundary identification. This results in better predicting the onset and duration of high-speed streams (HSSs). In addition, we find an optimized source surface height ($R_{ss}$) (lying between 1.8-3.1 $R_{\odot}$) further enhances HSS prediction accuracy for the studied events. A detailed analysis shows that changes in $R_{ss}$, (a) changes the Great Circle Angular Distance (GCAD) maps (at the solar surface) of the associated coronal holes and (b) changes the foot-point locations of the magnetic connectivities to the sub-Earth locations. These factors change the near-Sun SW speed, that eventually leads to uncertainties in speeds near Earth. We also investigate the usefulness of coronal hole observations in constraining $R_{ss}$ and SW solutions at Earth, and highlight their underutilized value in guiding the selection of magnetic maps for improved ambient solar wind modeling at L1.

Addressing this crucial aspect, studies in the past have shown that possible sources of error could include the choice of the input magnetic maps (Riley et al. 2012; Gressl et al. 2014; Riley et al. 2014; Li et al. 2021; Jin et al. 2022; Demidov et al. 2023; Perri et al. 2023; Wang & Samara 2024), pre-processing of magnetic maps (Tóth et al. 2011) and the choice of the coronal models themselves (Tóth et al. 2011; Gressl et al. 2014; Jian et al. 2015; MacNeice et al. 2018; Jones et al. 2024; Asvestari et al. 2024).

Demidov, M. L., Hanaoka, Y., Wang, X. F., & Kirichkov, P. N. 2023, SoPh, 298, 120, doi: 10.1007/s11207-023-02206-6

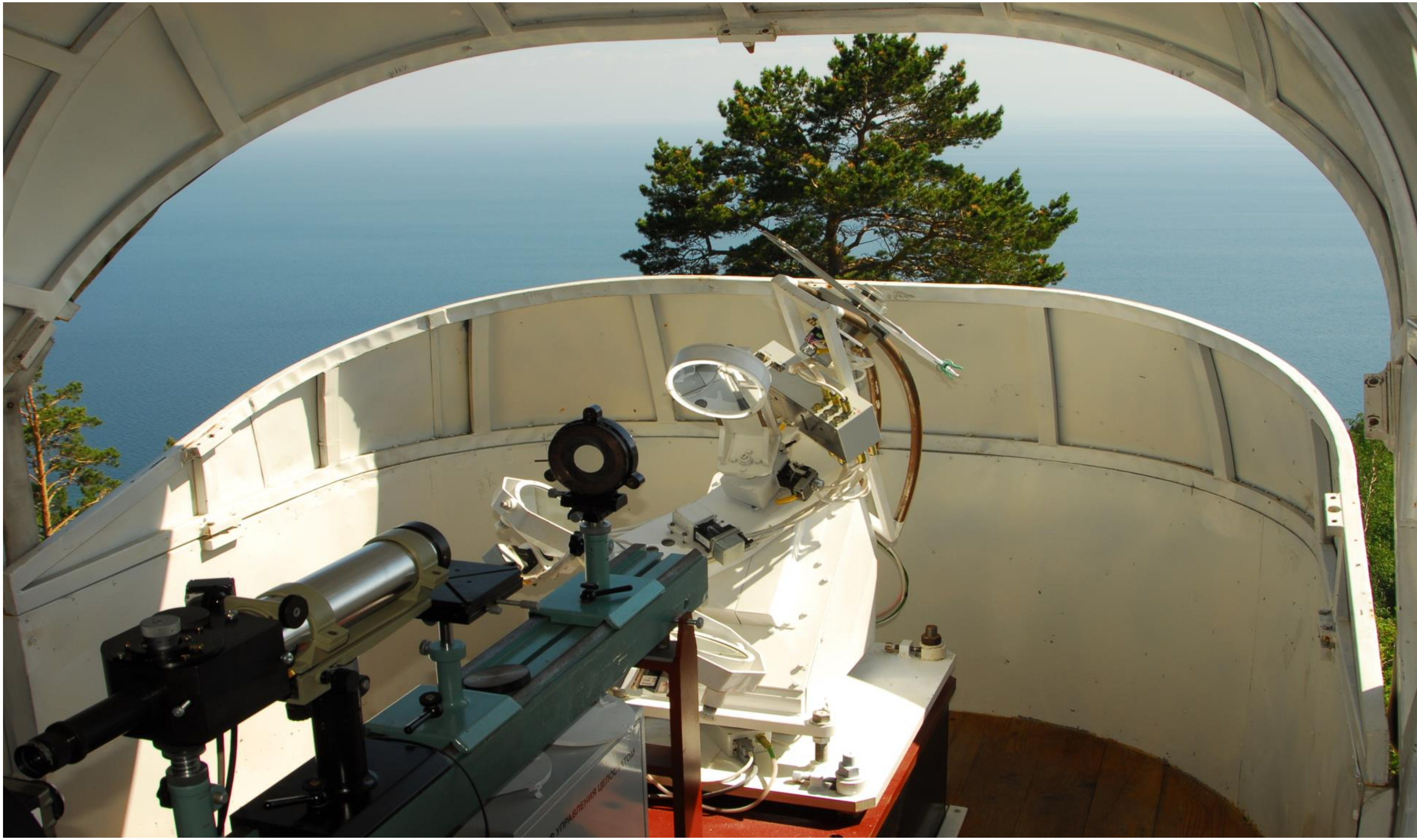

УДК 520.24; 681.51

# СОЛНЕЧНЫЙ ТЕЛЕСКОП ОПЕРАТИВНЫХ ПРОГНОЗОВ НОВОГО ПОКОЛЕНИЯ*

**В. С. Пещеров[1], В. М. Григорьев[1], П. М. Свидский[2], А. Н. Бевзов[3], К. И. Будников[3], С. В. Власов[3], А. А. Зотов[3], В. Н. Котов[3], А. К. Китов[1], А. А. Лубков[3], С. А. Лылов[3], С. В. Перебейнос[3]**

[1]*Институт солнечно-земной физики СО РАН,*
*664033, г. Иркутск, ул. Лермонтова, 126а, а/я 291*
*E-mail: vsp@iszf.irk.ru*
[2]*Институт прикладной геофизики им. академика Е. К. Федорова,*
*129128, Москва, ул. Ростокинская, 9*
*E-mail: svidsky@mail.ru*
[3]*Институт автоматики и электрометрии СО РАН,*
*630090, г. Новосибирск, просп. Академика Коптюга, 1*
*E-mail: lubkov@iae.nsk.su*

Рассматриваются функциональные и метрологические характеристики нового солнечного телескопа, предназначенного для получения количественных данных о крупномасштабных магнитных полях (КМП) Солнца. Полная автоматизация процесса измерений, применение ПЗС-матриц в системах сканирования изображения и регистрации спектров и оптическая схема, согласованная с основной задачей телескопа, привели к существенному повышению оперативности, качества, точности измерений КМП и расширению круга задач в сравнении с существующими телескопами. Созданная автоматизированная система управления телескопом, измерительная система и программа обработки результатов измерений в реальном времени позволяют получать магнитограмму КМП с требуемой точностью за время около 15 мин.

*Ключевые слова:* телескоп, автоматизированная система управления, измерения КМП, Солнце, магнитограмма.

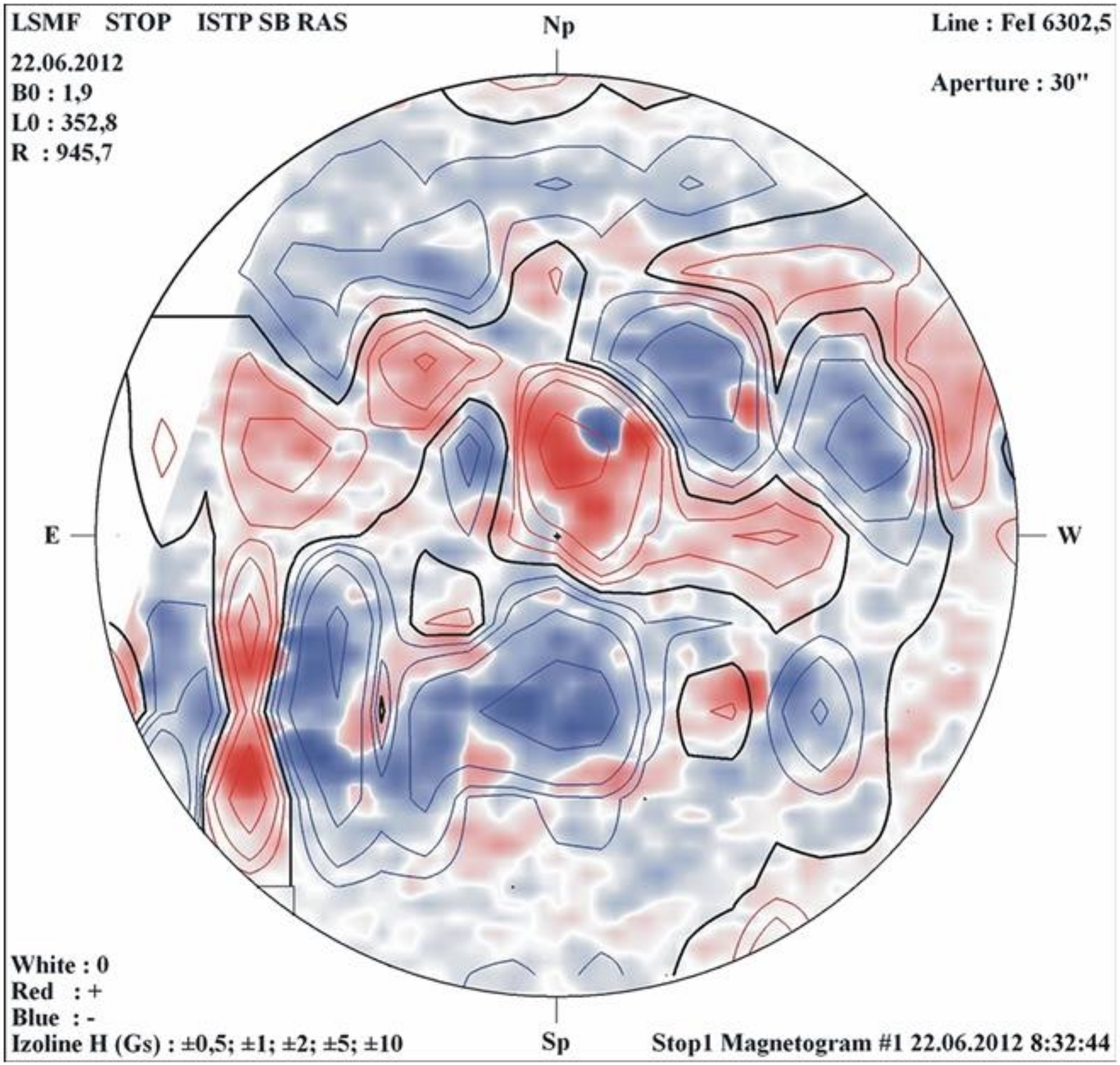
LSMF STOP ISTP SB RAS
22.06.2012
B0 : 1,9
L0 : 352,8
R : 945,7
Np
Line : FeI 6302,5
Aperture : 30"
E
W
White : 0
Red : +
Blue : -
Izoline H (Gs) : ±0,5; ±1; ±2; ±5; ±10
Sp
Stop1 Magnetogram #1 22.06.2012 8:32:44

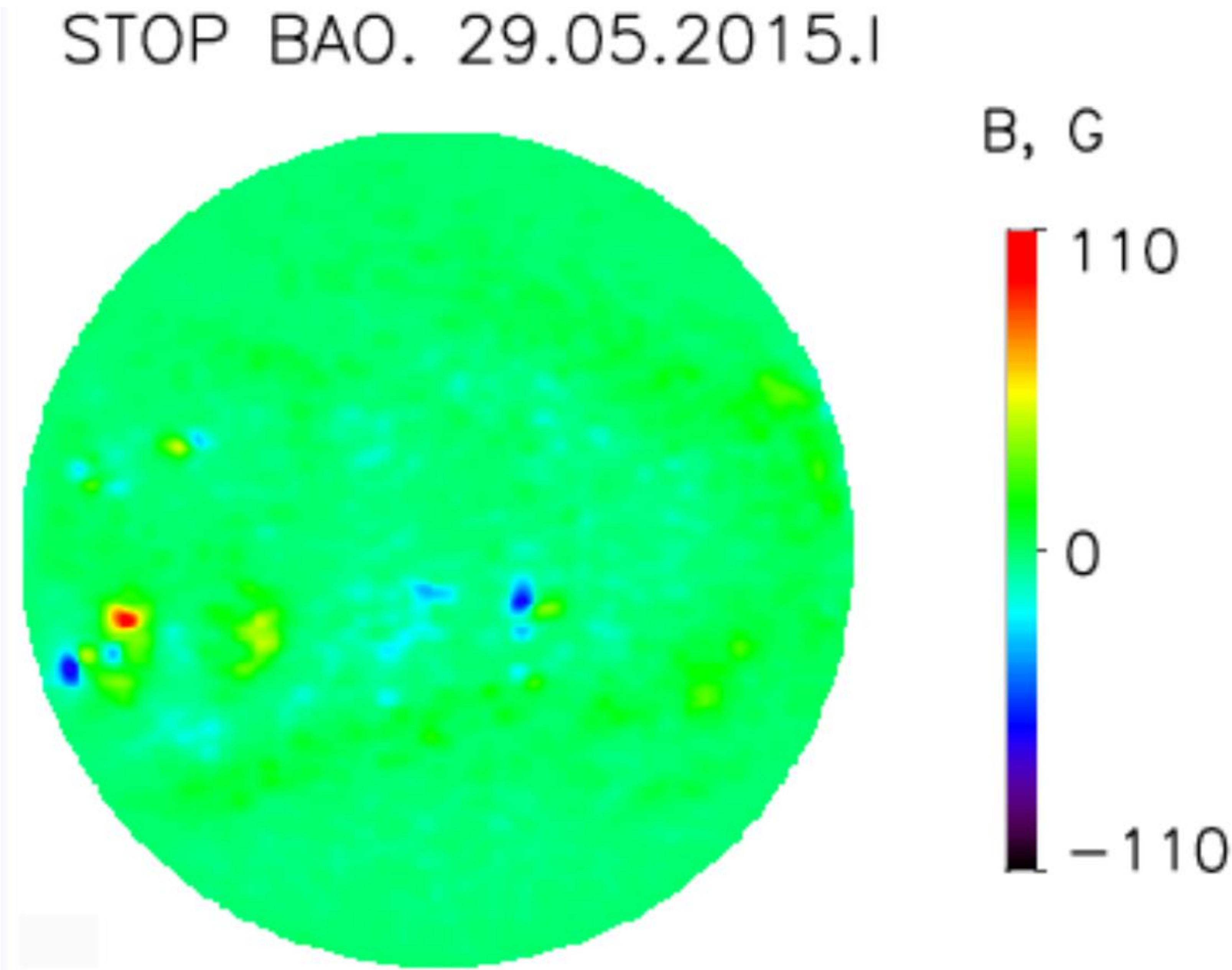
STOP BAO. 29.05.2015.I
B, G
110
0
−110

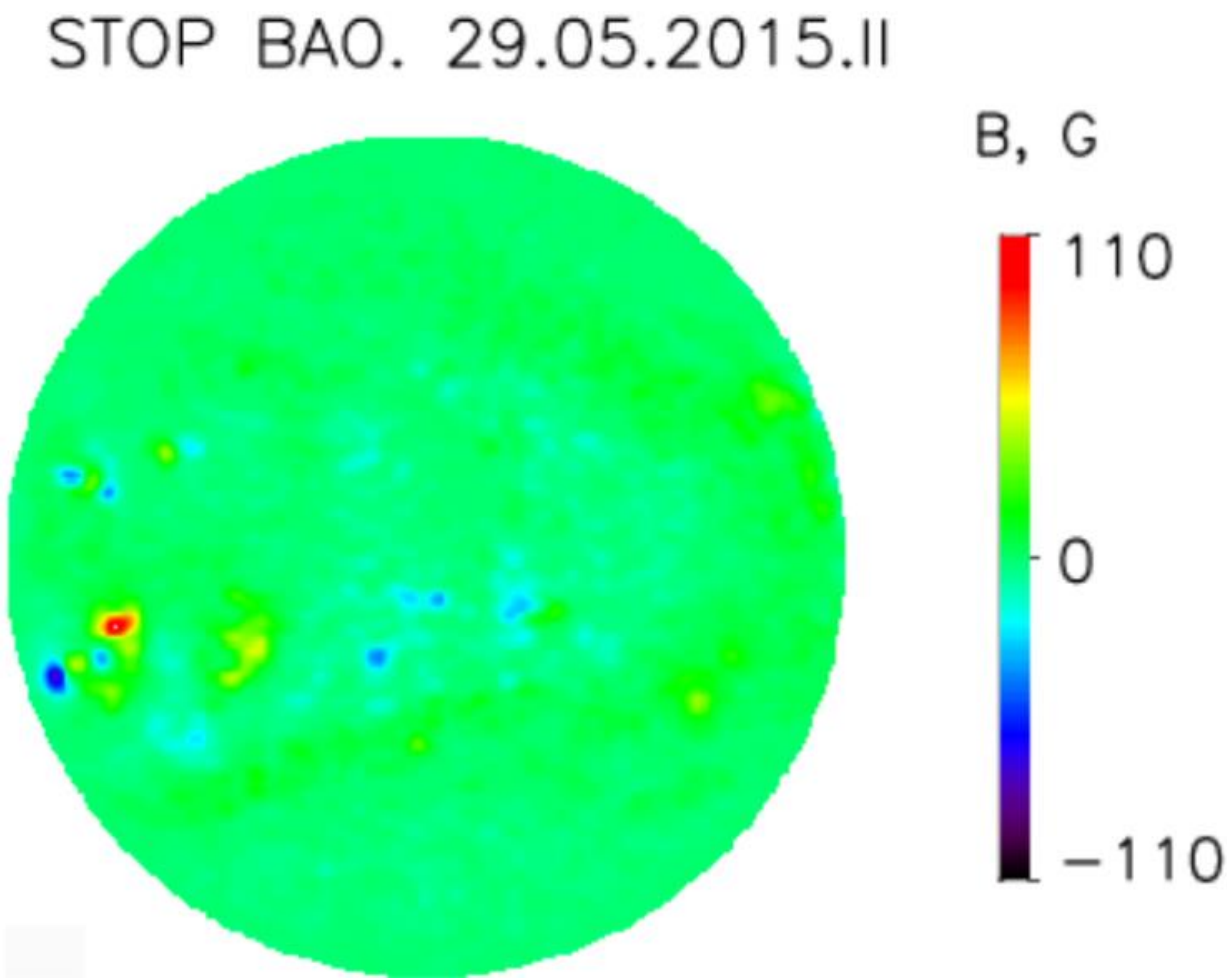

STOP BAO. 29.05.2015.II
B, G
110
0
−110

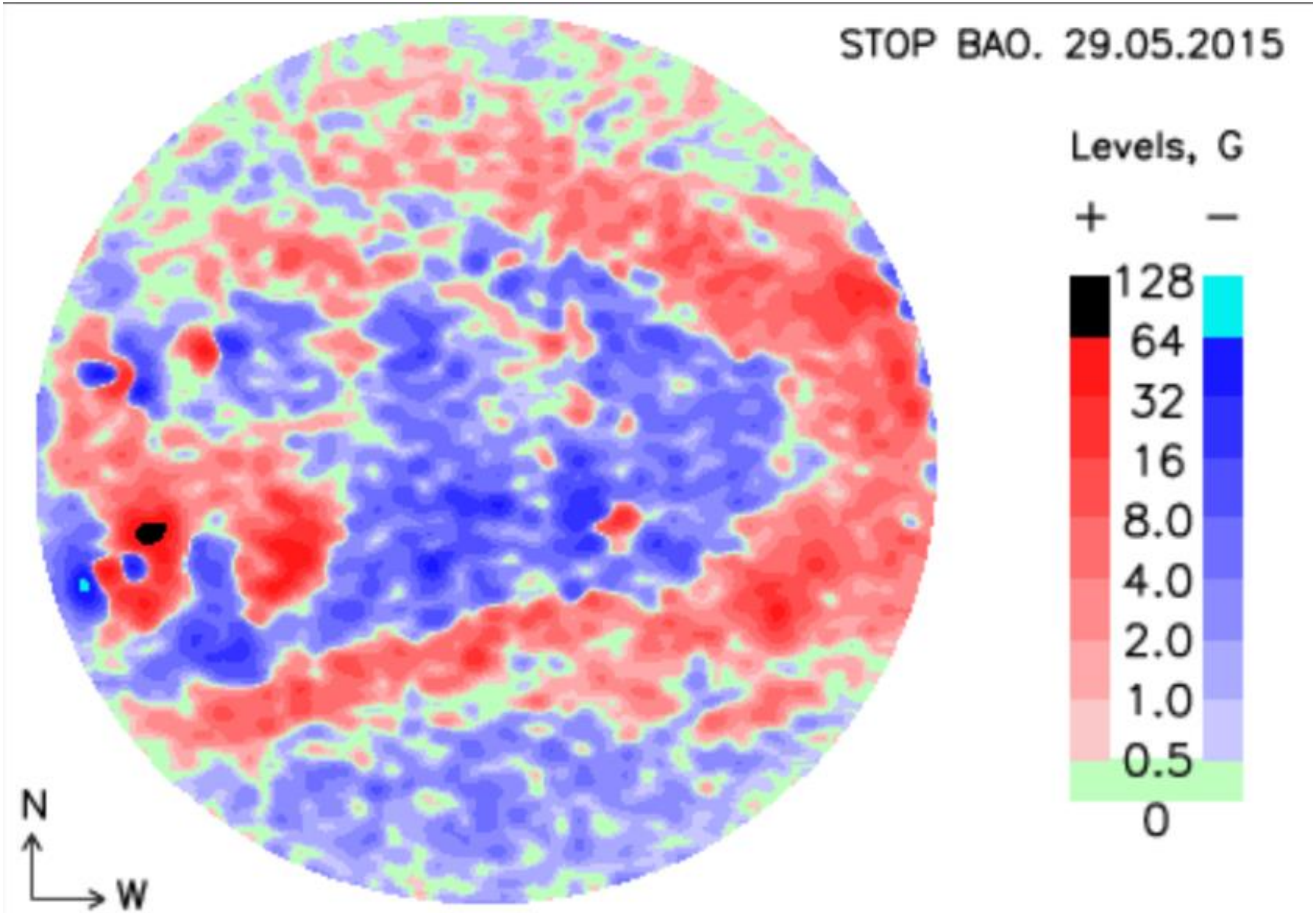
STOP BAO. 29.05.2015
Levels, G
+
−
128
64
32
16
8.0
4.0
2.0
1.0
0.5
0
N
W

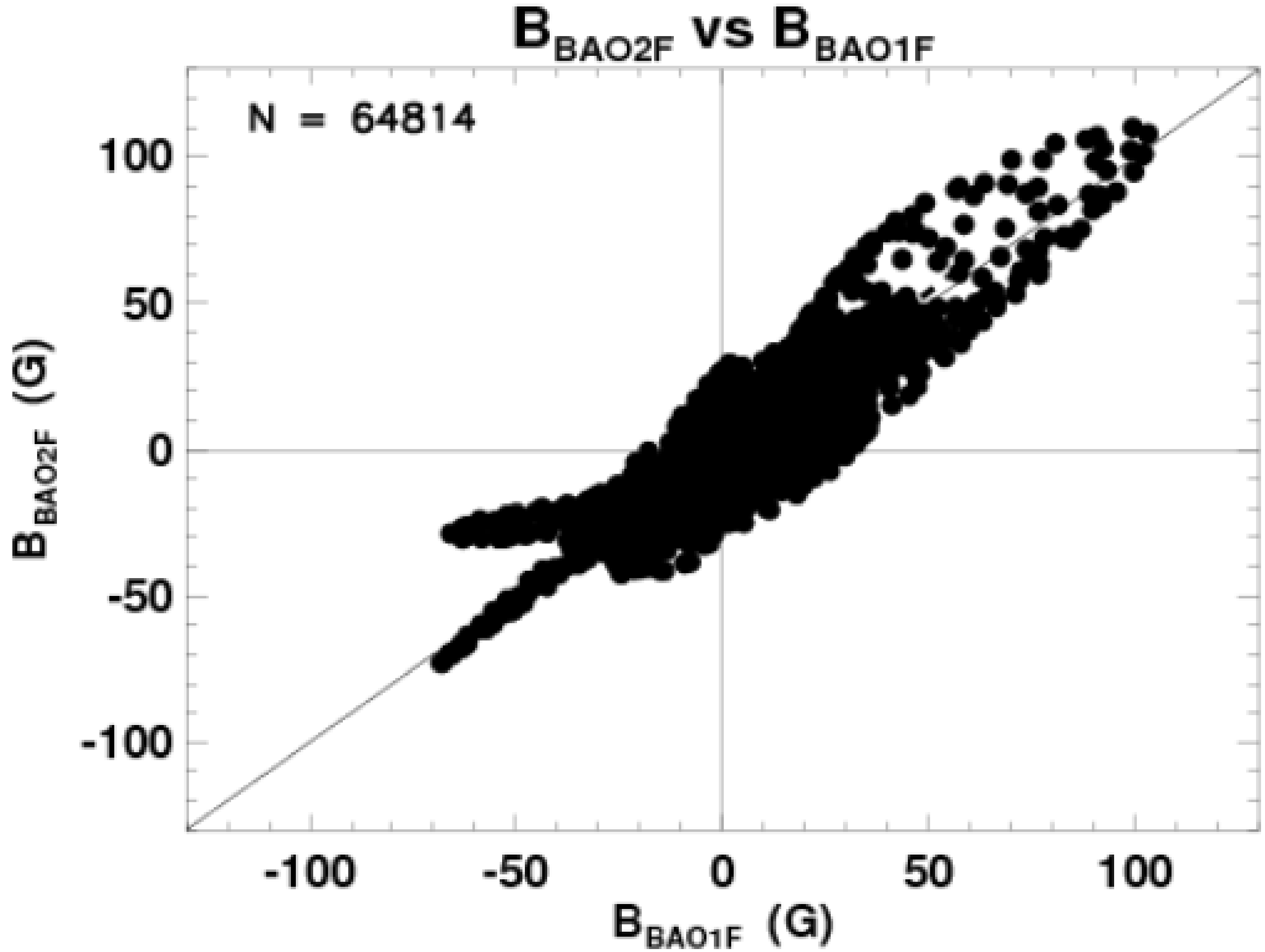

$B_{BAO2F}$ vs $B_{BAO1F}$
N = 64814
100
50
0
-50
-100
$B_{BAO2F}$ (G)
-100
-50
0
50
100
$B_{BAO1F}$ (G)

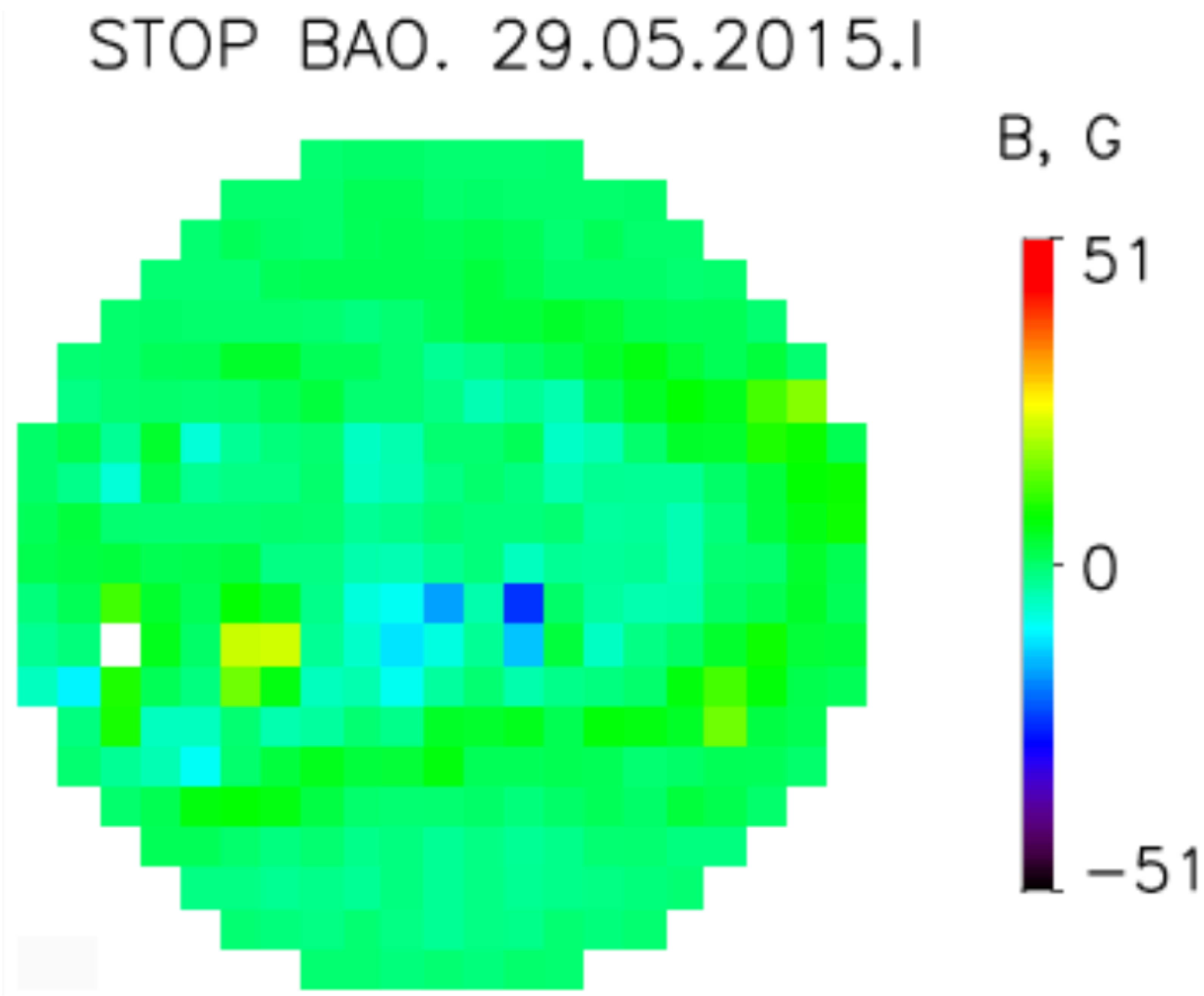
STOP BAO. 29.05.2015.I
B, G
51
0
−51

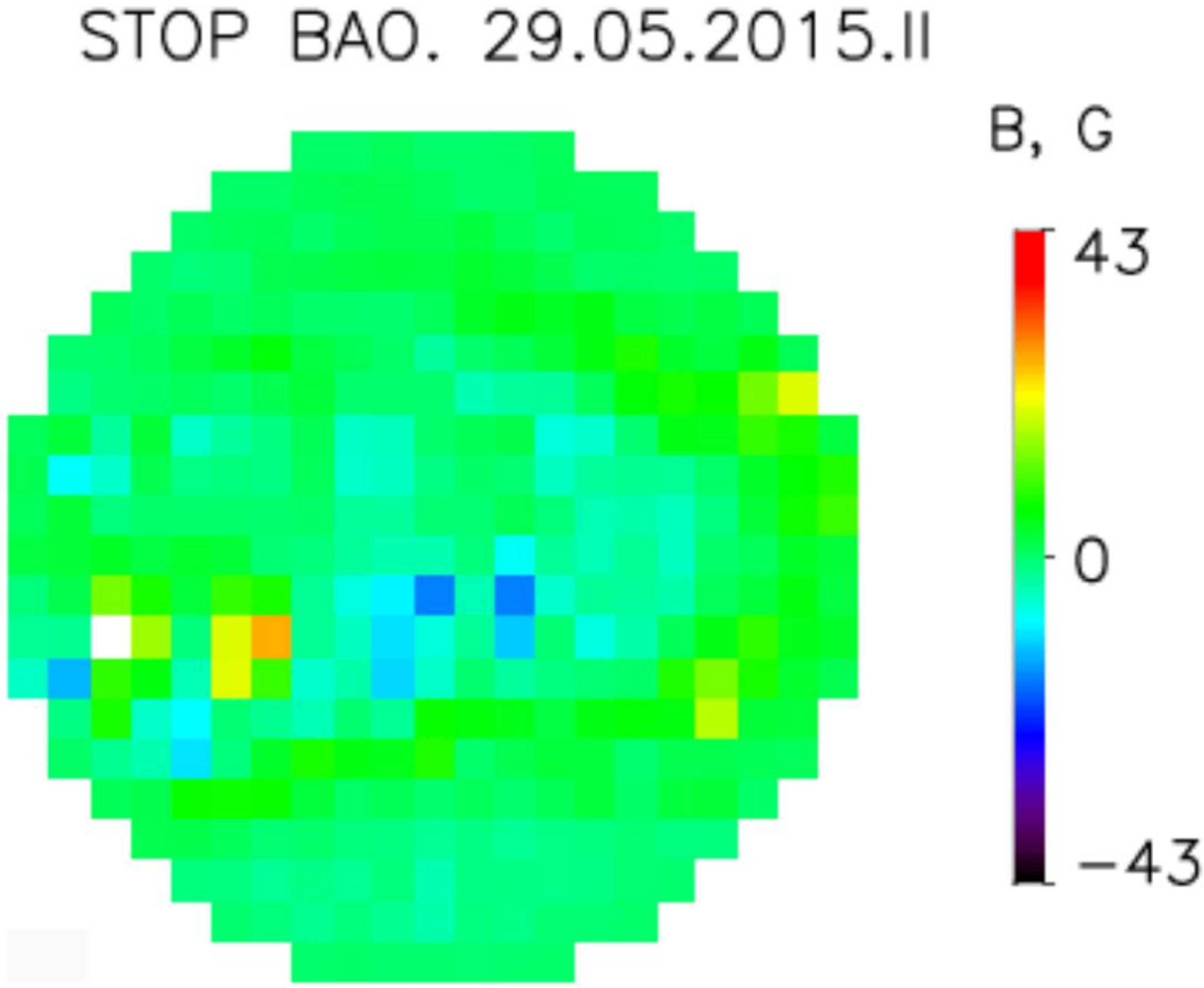
STOP BAO. 29.05.2015.II
B, G
43
0
−43

STOP BAO.29.05.2015.I

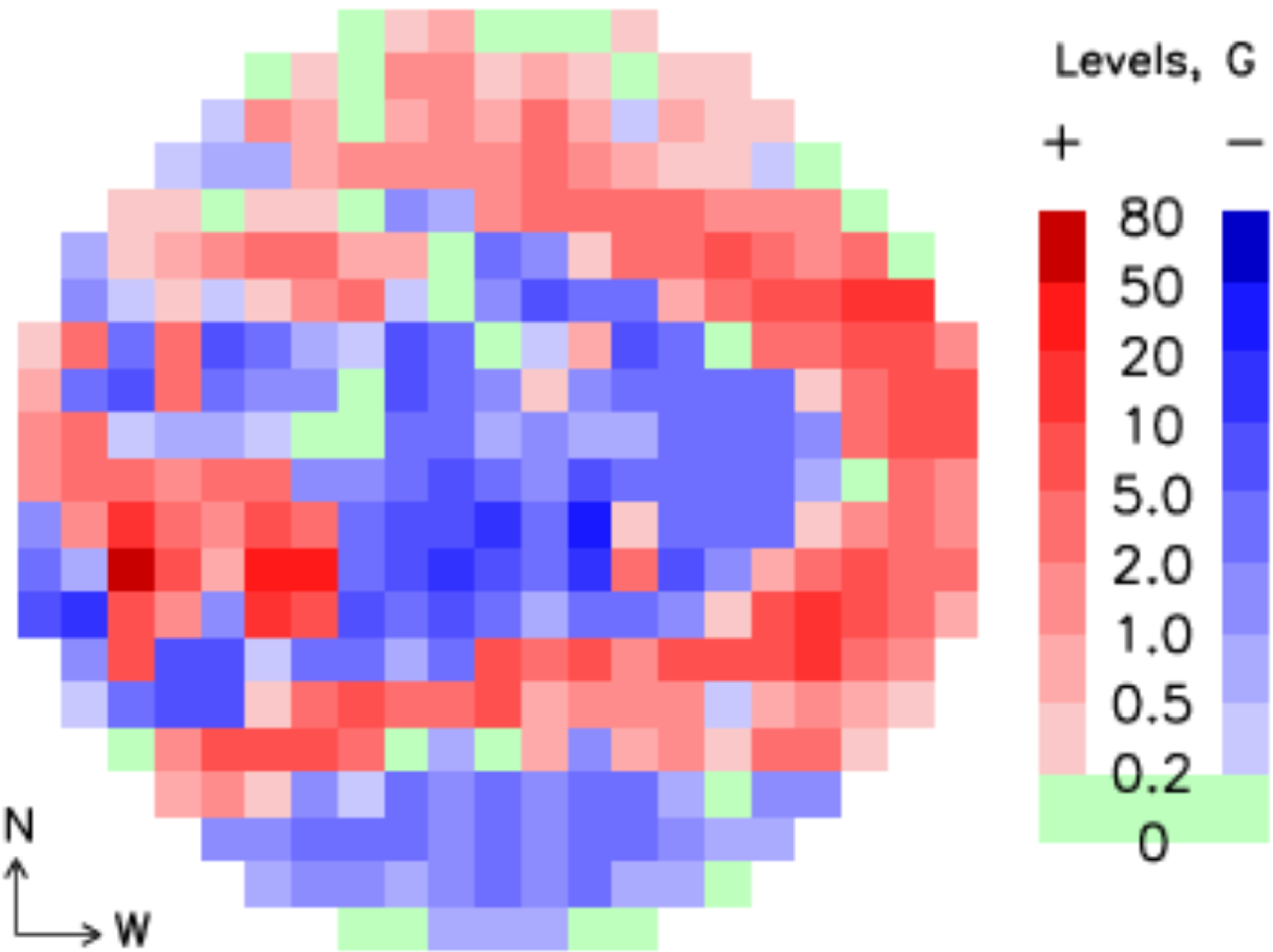

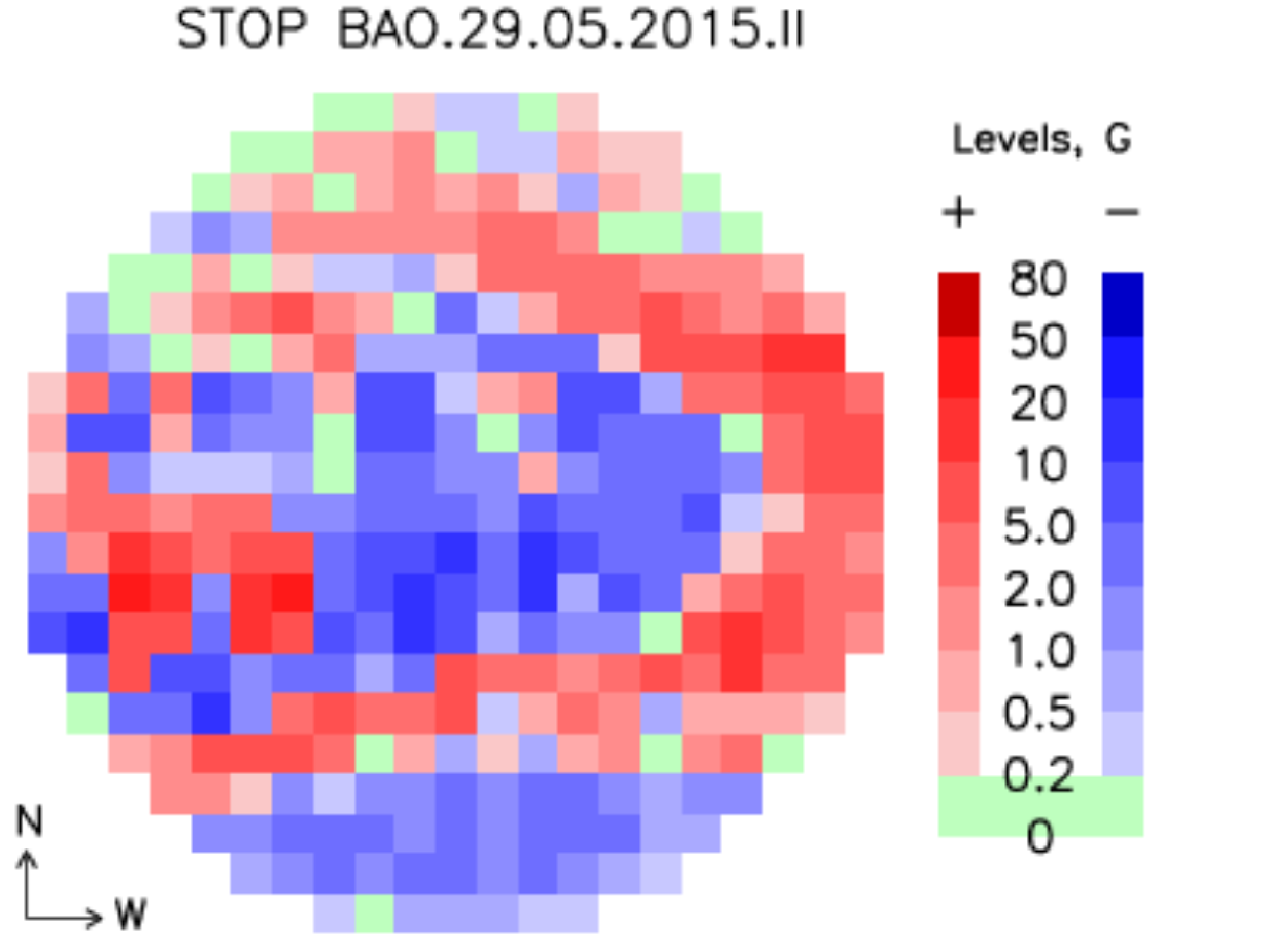

STOP BAO.29.05.2015.II
Levels, G
+
−
80
50
20
10
5.0
2.0
1.0
0.5
0.2
0
N
W

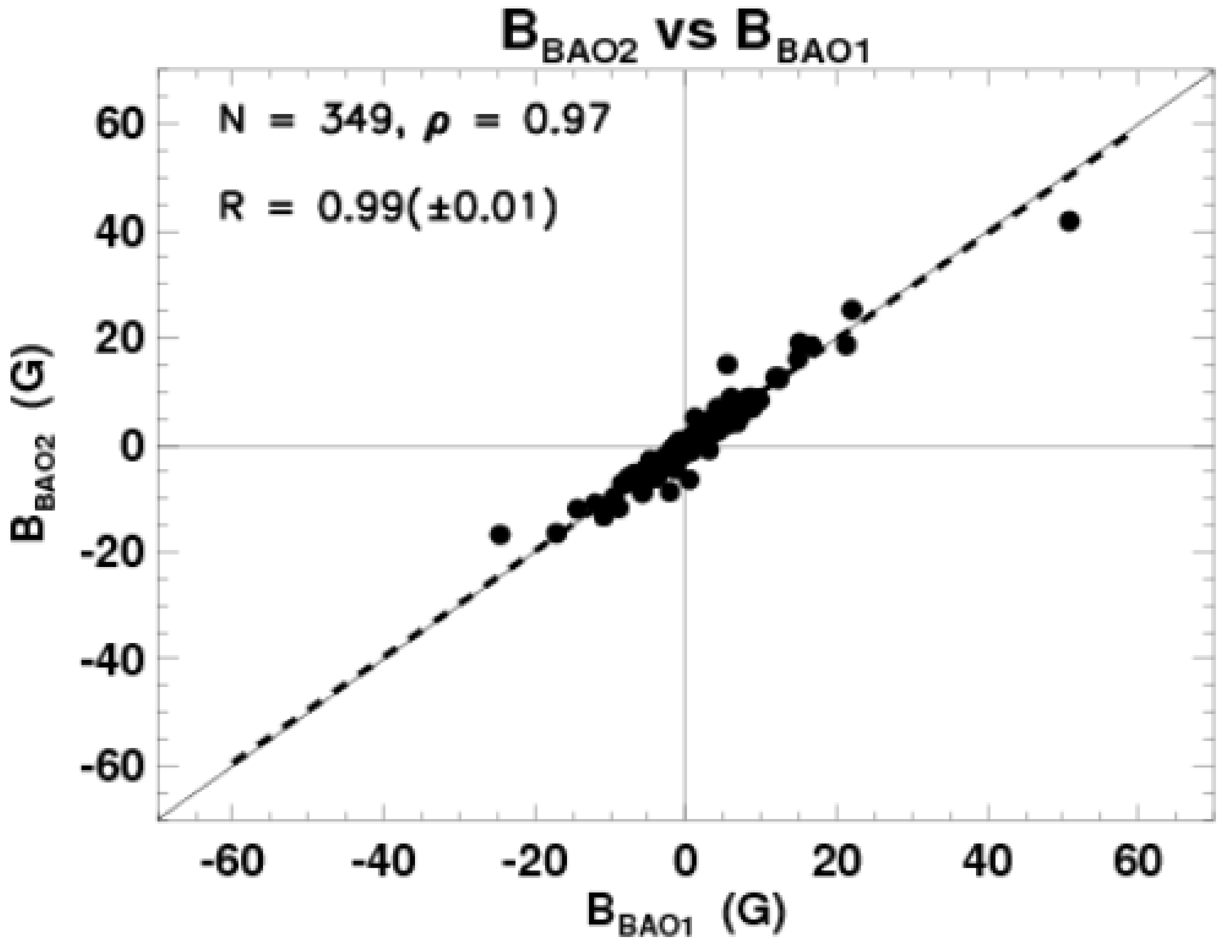

B_BAO2 vs B_BAO1
N = 349, ρ = 0.97
R = 0.99(±0.01)
B_BAO2 (G)
B_BAO1 (G)
60
40
20
0
-20
-40
-60

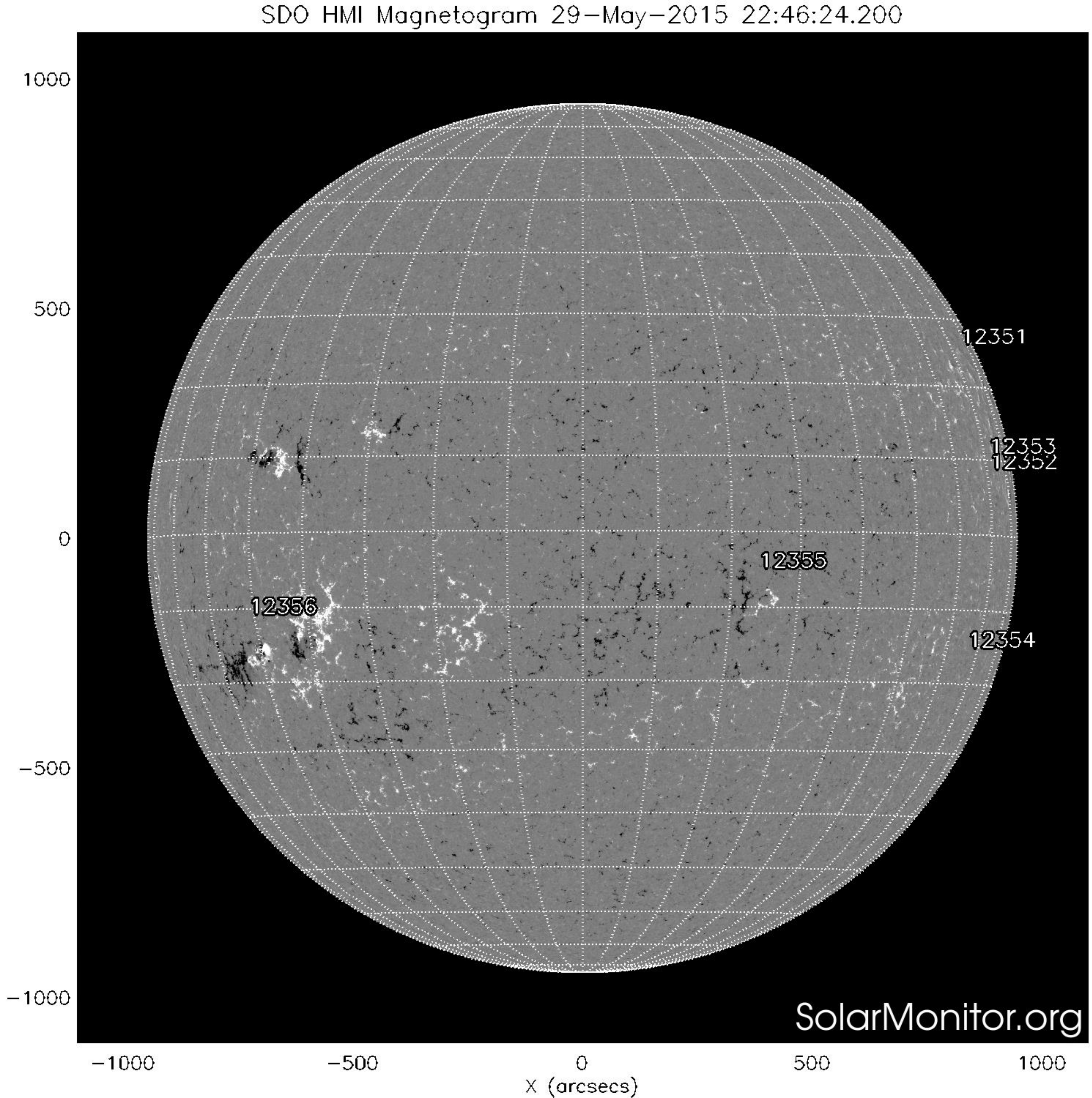
SDO HMI Magnetogram 29-May-2015 22:46:24.200
1000
500
0
−500
−1000
−1000
−500
0
500
1000
X (arcsecs)
12351
12353
12352
12355
12356
12354
SolarMonitor.org

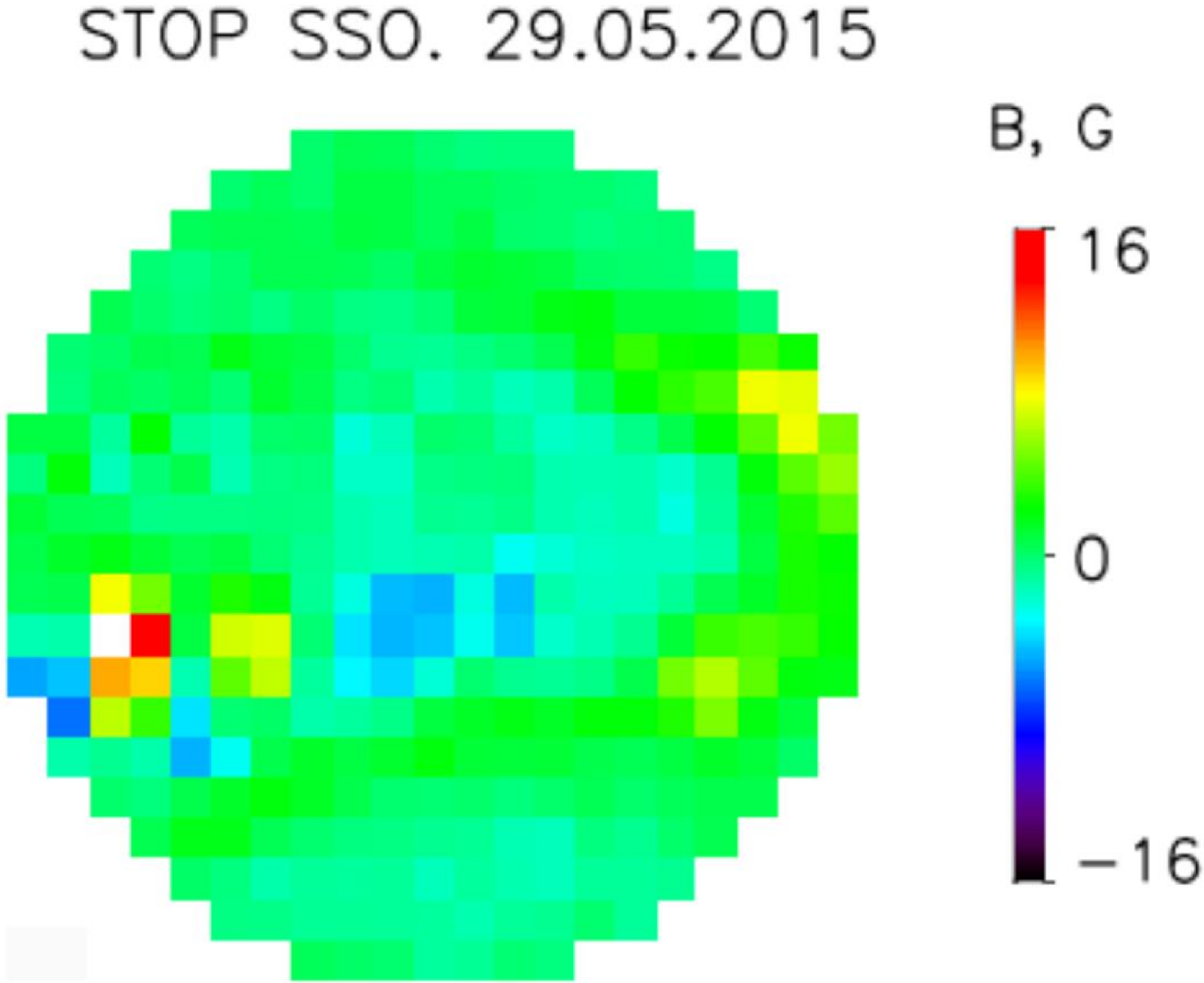
STOP SSO. 29.05.2015
B, G
16
0
−16

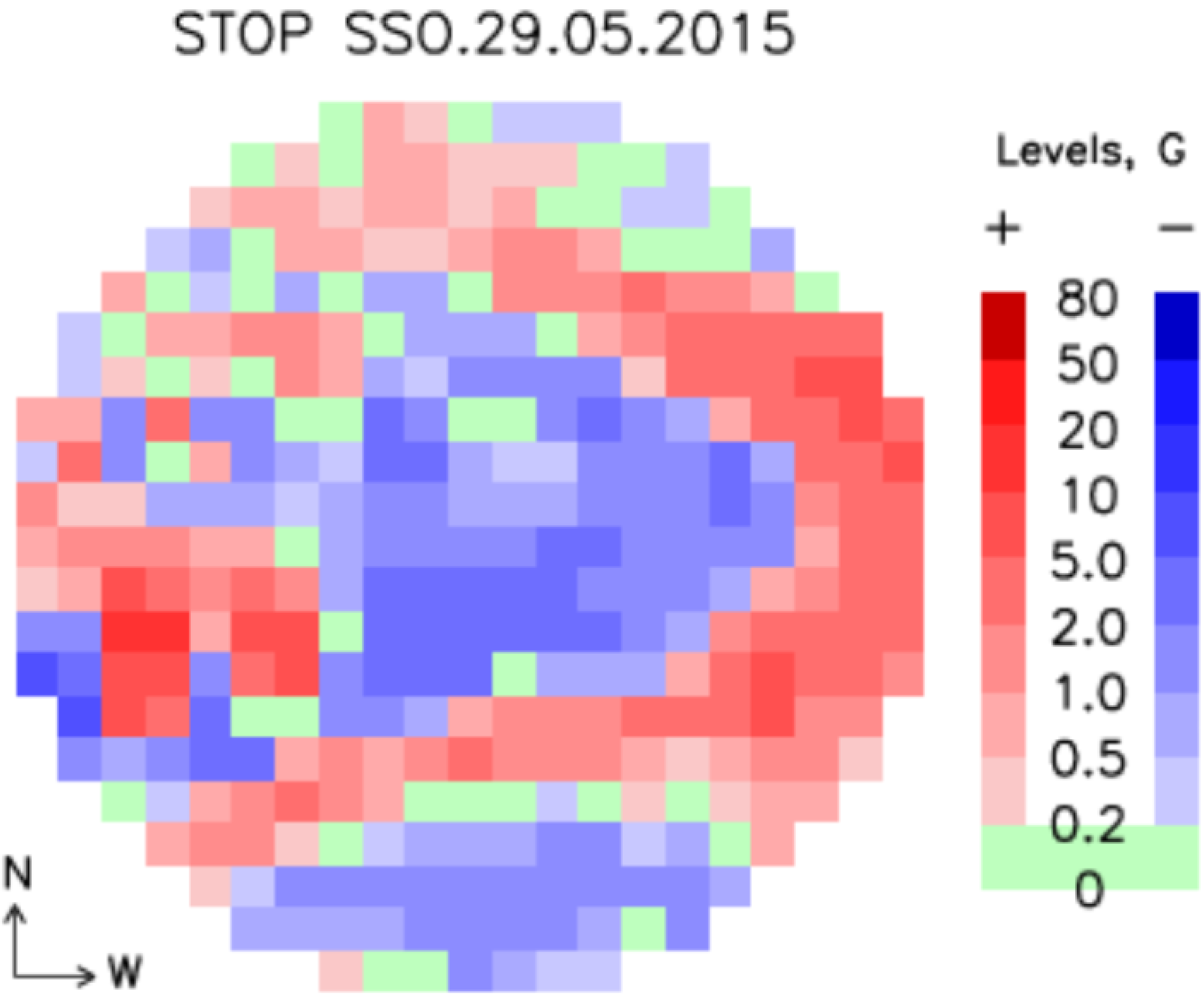
STOP SSO.29.05.2015
Levels, G
+
−
80
50
20
10
5.0
2.0
1.0
0.5
0.2
0
N
W

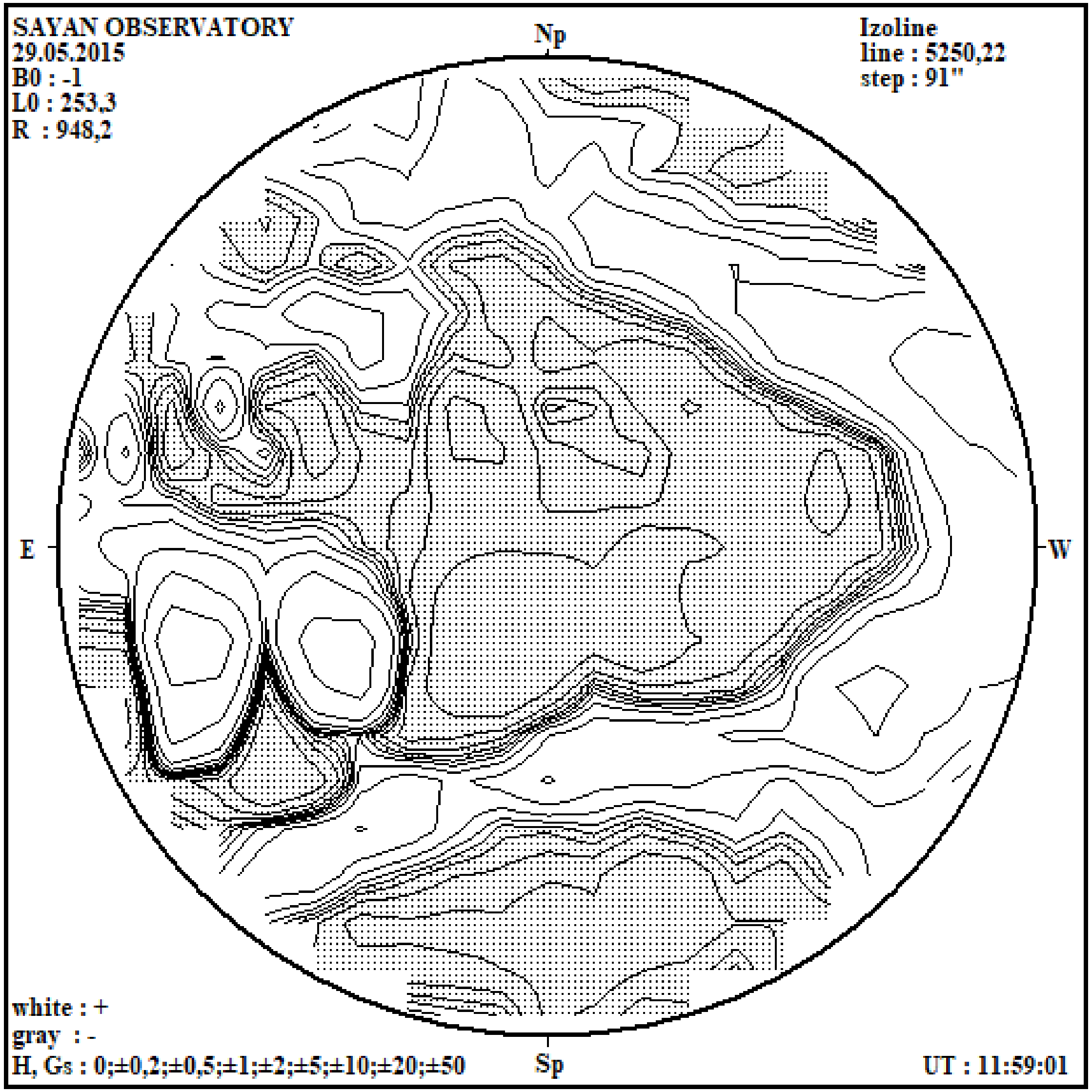

SAYAN OBSERVATORY
29.05.2015
B0 : -1
L0 : 253,3
R : 948,2
Np
Izoline
line : 5250,22
step : 91"
E
W
white : +
gray : -
H, Gs : 0;±0,2;±0,5;±1;±2;±5;±10;±20;±50
Sp
UT : 11:59:01

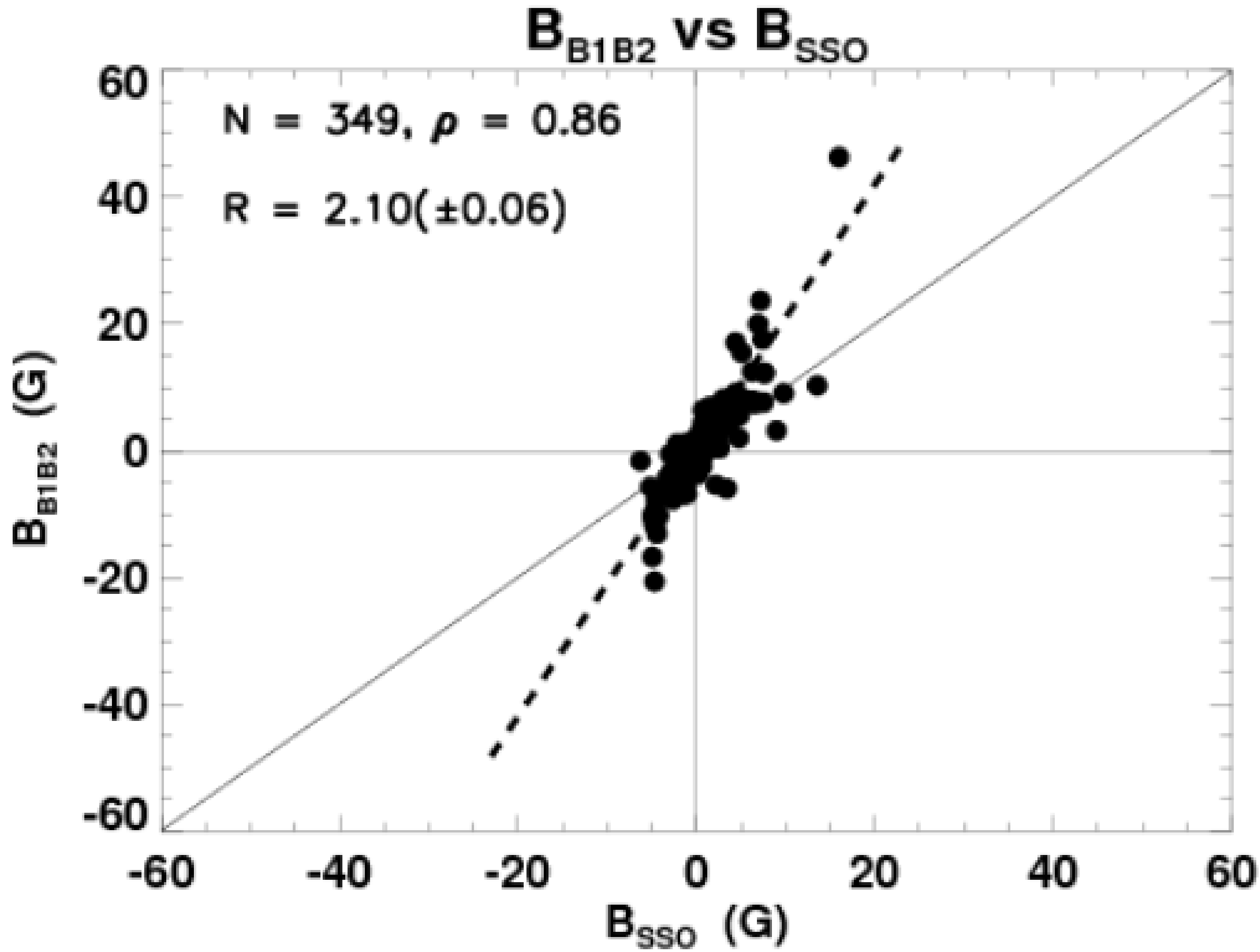

$B_{B1B2}$ vs $B_{SSO}$
N = 349, ρ = 0.86
R = 2.10(±0.06)
60
40
20
0
-20
-40
-60
$B_{B1B2}$ (G)
-60
-40
-20
0
20
40
60
$B_{SSO}$ (G)

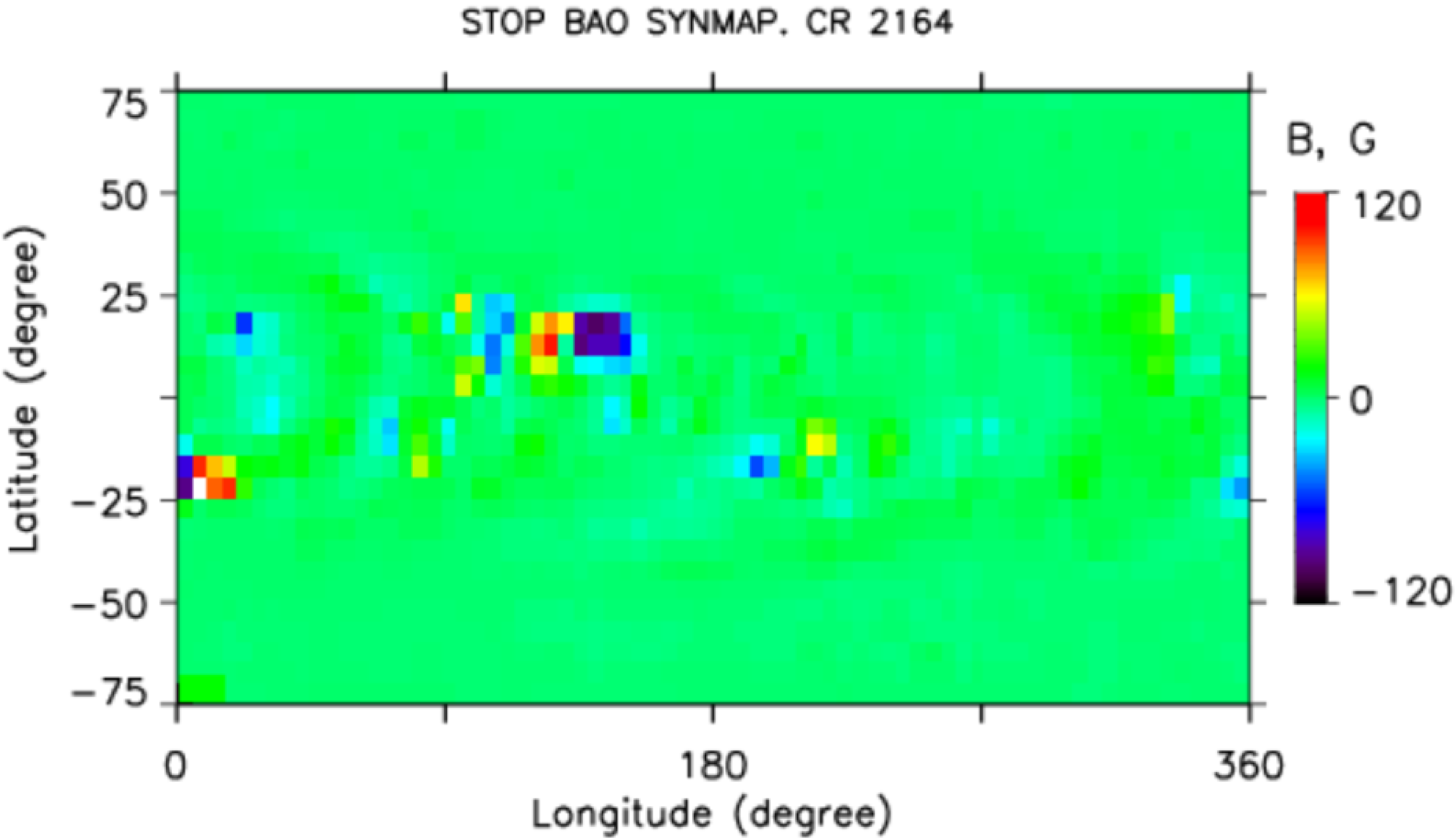
STOP BAO SYNMAP, CR 2164
B, G
120
0
−120
75
50
25
−25
−50
−75
Latitude (degree)
0
180
360
Longitude (degree)

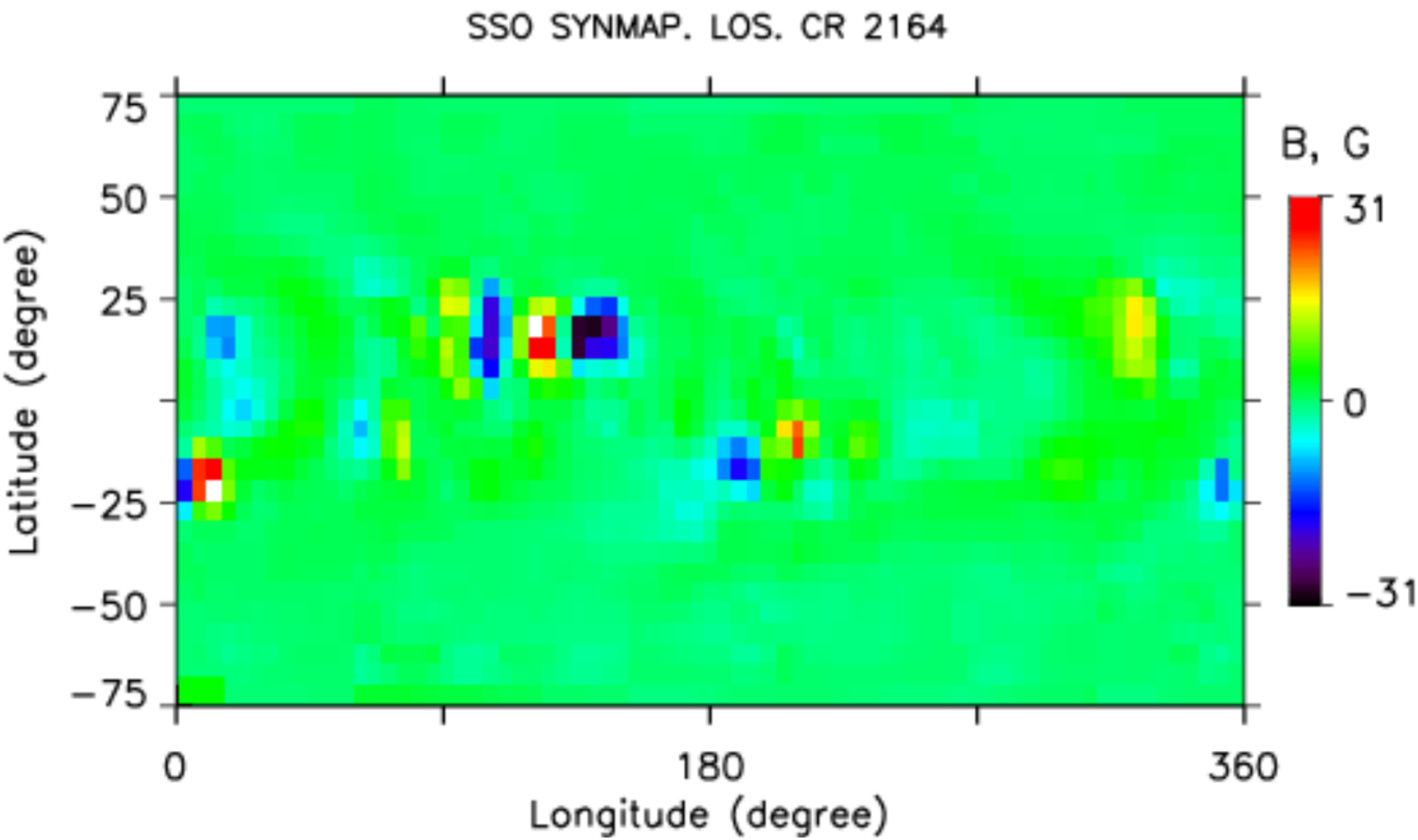
SSO SYNMAP. LOS. CR 2164
B, G
31
0
−31
75
50
25
−25
−50
−75
Latitude (degree)
0
180
360
Longitude (degree)

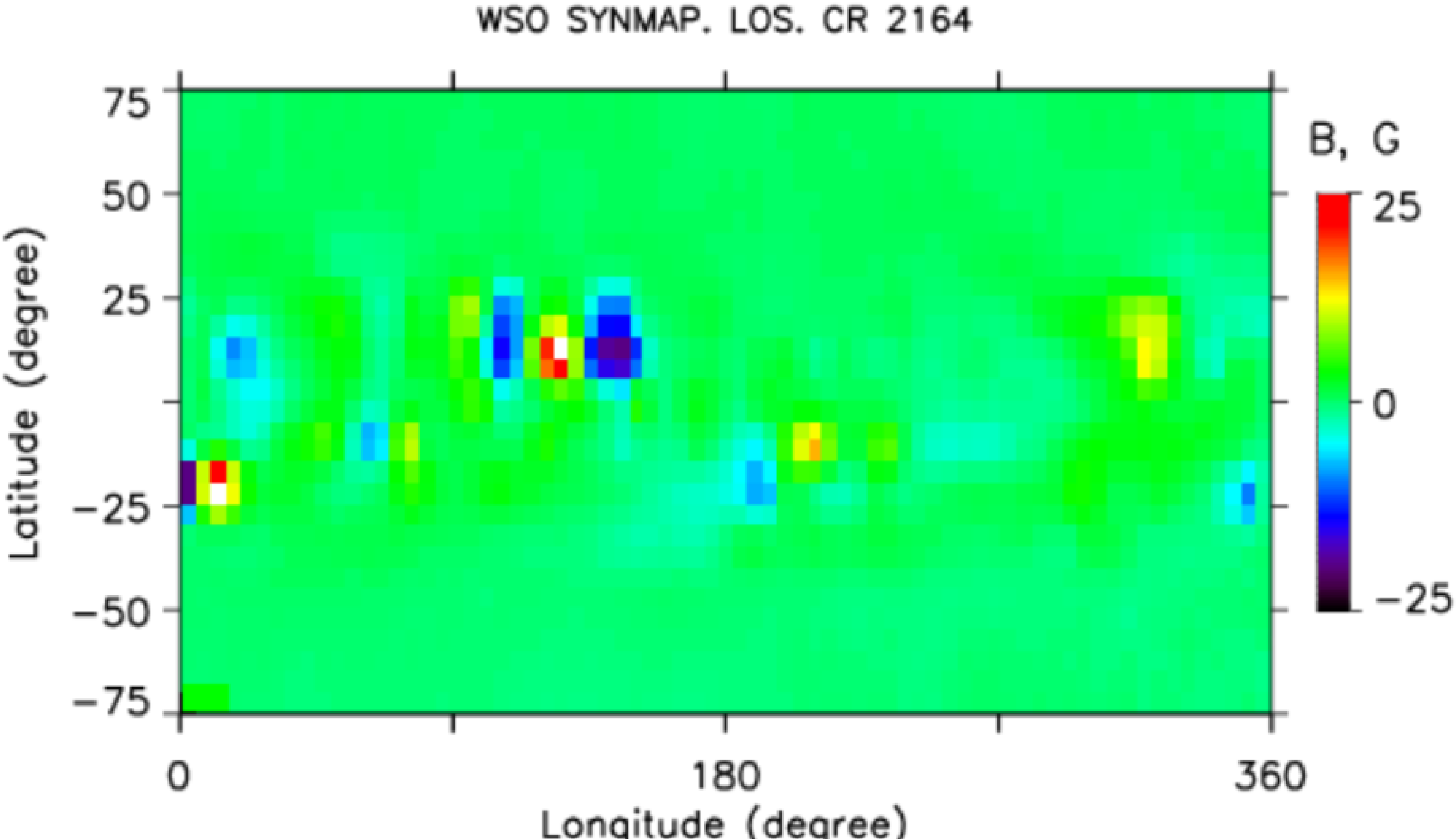
WSO SYNMAP. LOS. CR 2164
B, G
25
0
−25
75
50
25
−25
−50
−75
Latitude (degree)
0
180
360
Longitude (degree)

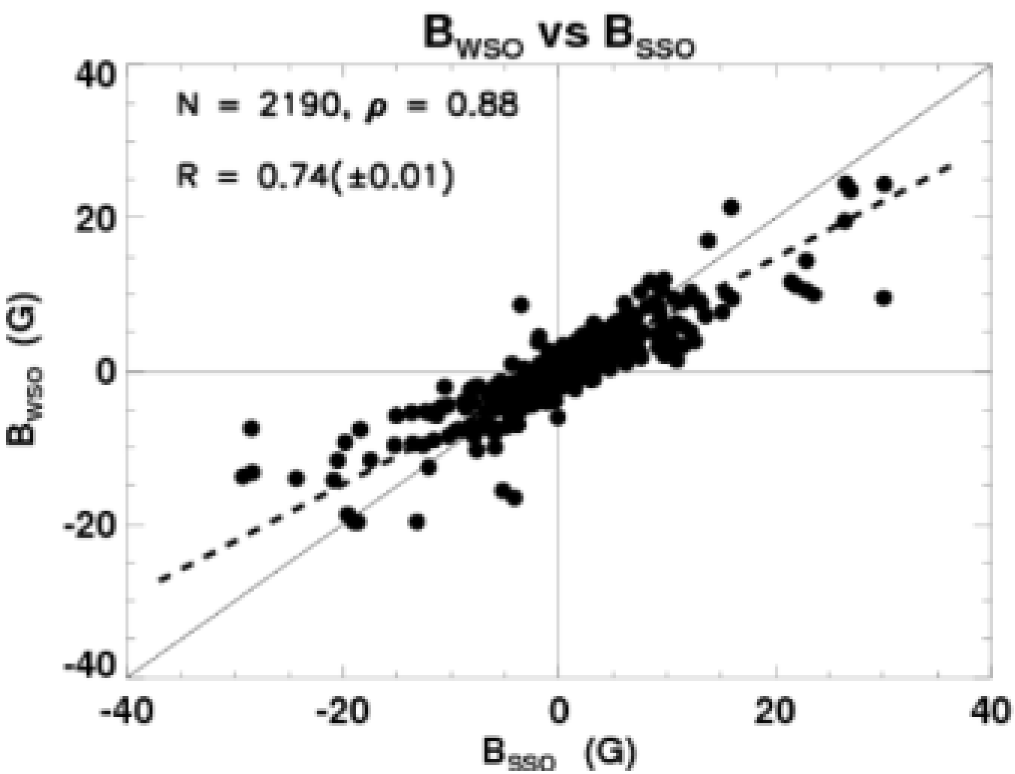

B_WSO vs B_SSO
N = 2190, ρ = 0.88
R = 0.74(±0.01)
40
20
0
-20
-40
B_WSO (G)
-40
-20
0
20
40
B_SSO (G)

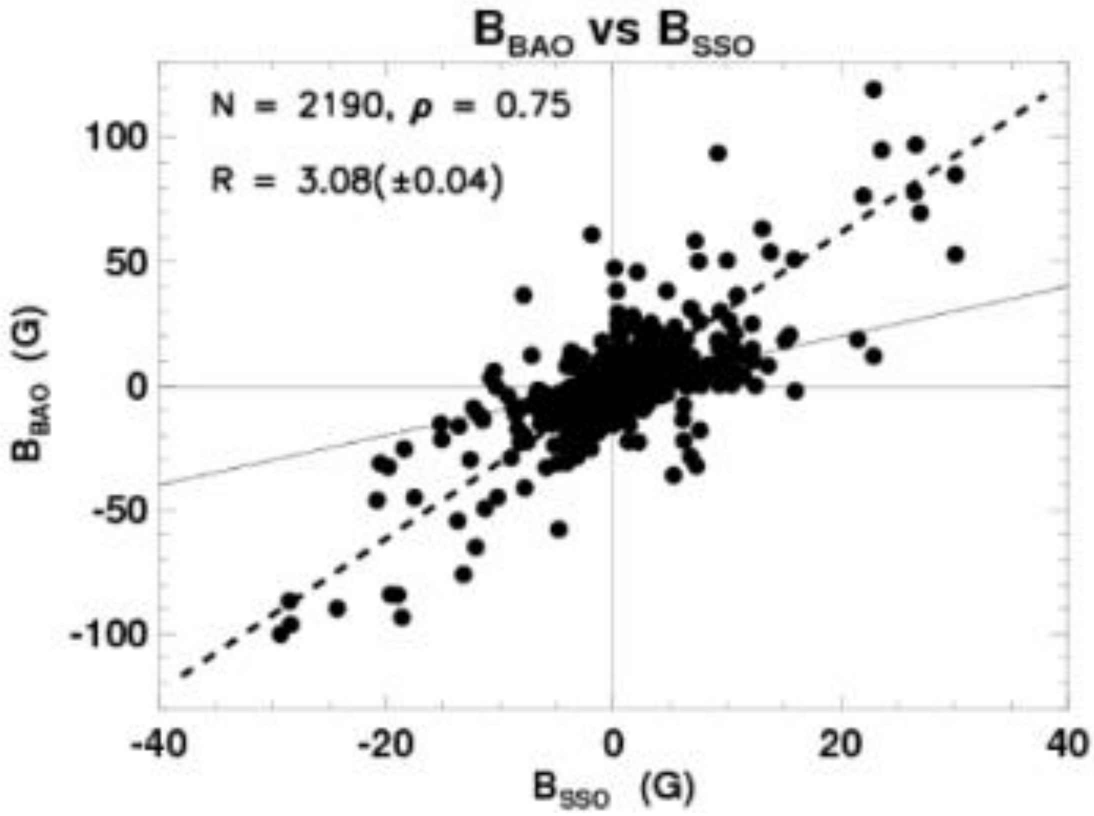
$B_{BAO}$ vs $B_{SSO}$
N = 2190, $\rho$ = 0.75
R = 3.08(±0.04)
100
50
0
-50
-100
$B_{BAO}$ (G)
-40
-20
0
20
40
$B_{SSO}$ (G)

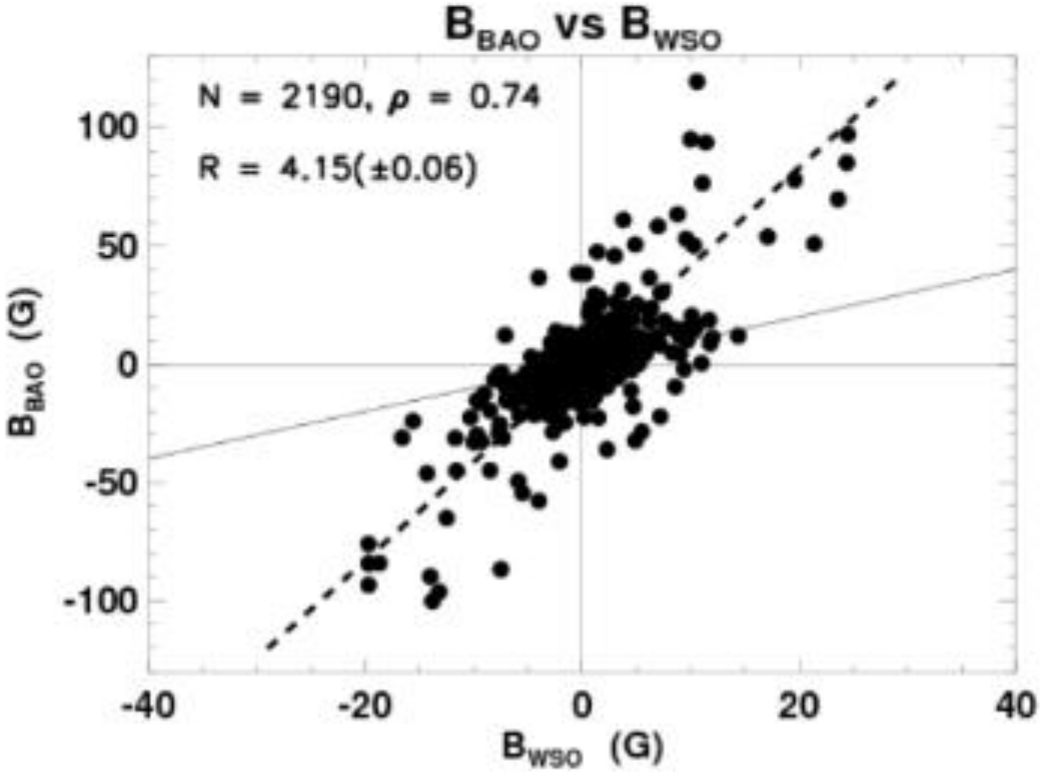
B_BAO vs B_WSO
N = 2190, ρ = 0.74
R = 4.15(±0.06)
100
50
0
-50
-100
B_BAO (G)
-40
-20
0
20
40
B_WSO (G)

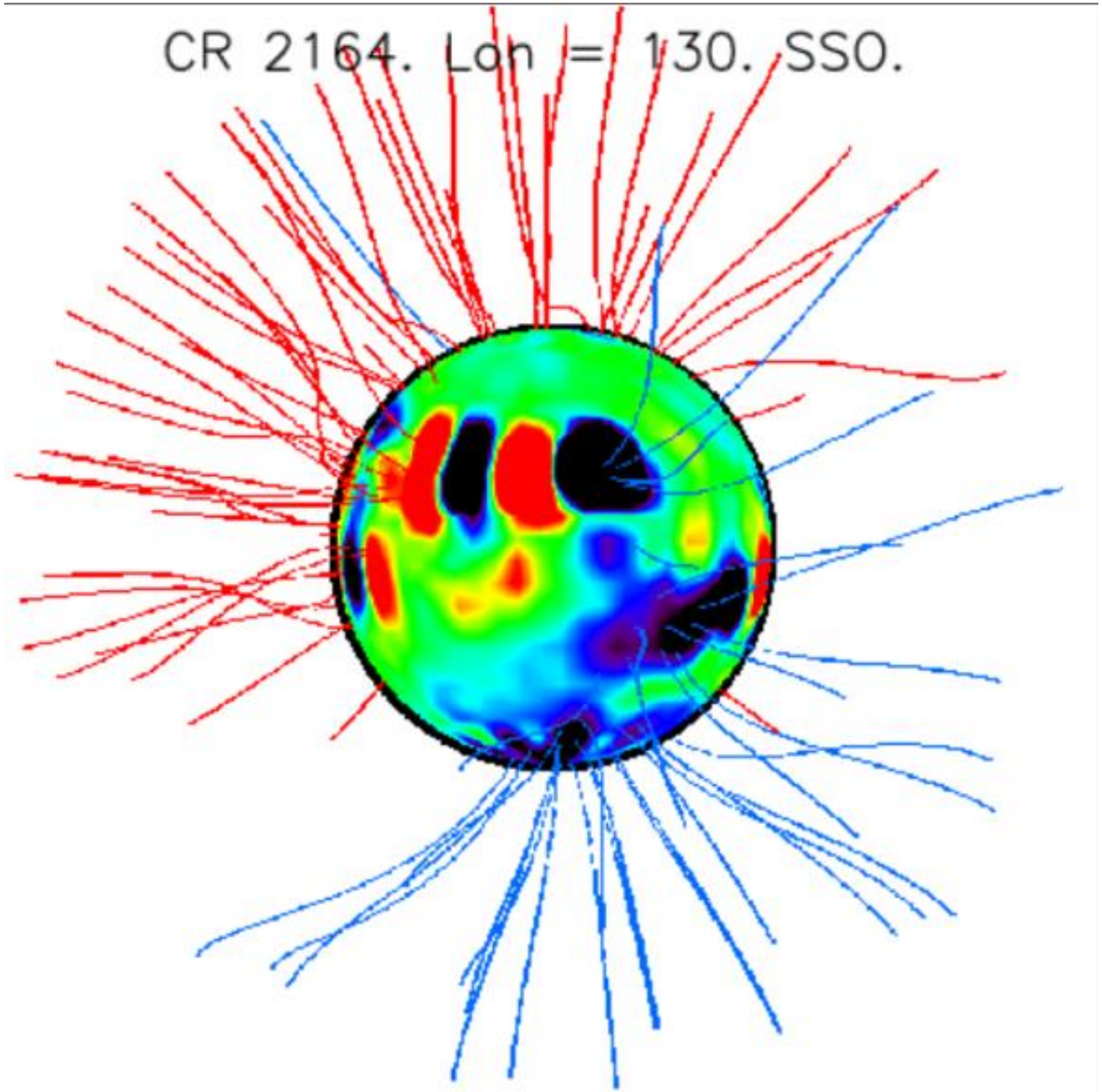
CR 2164. Lon = 130. SSO.

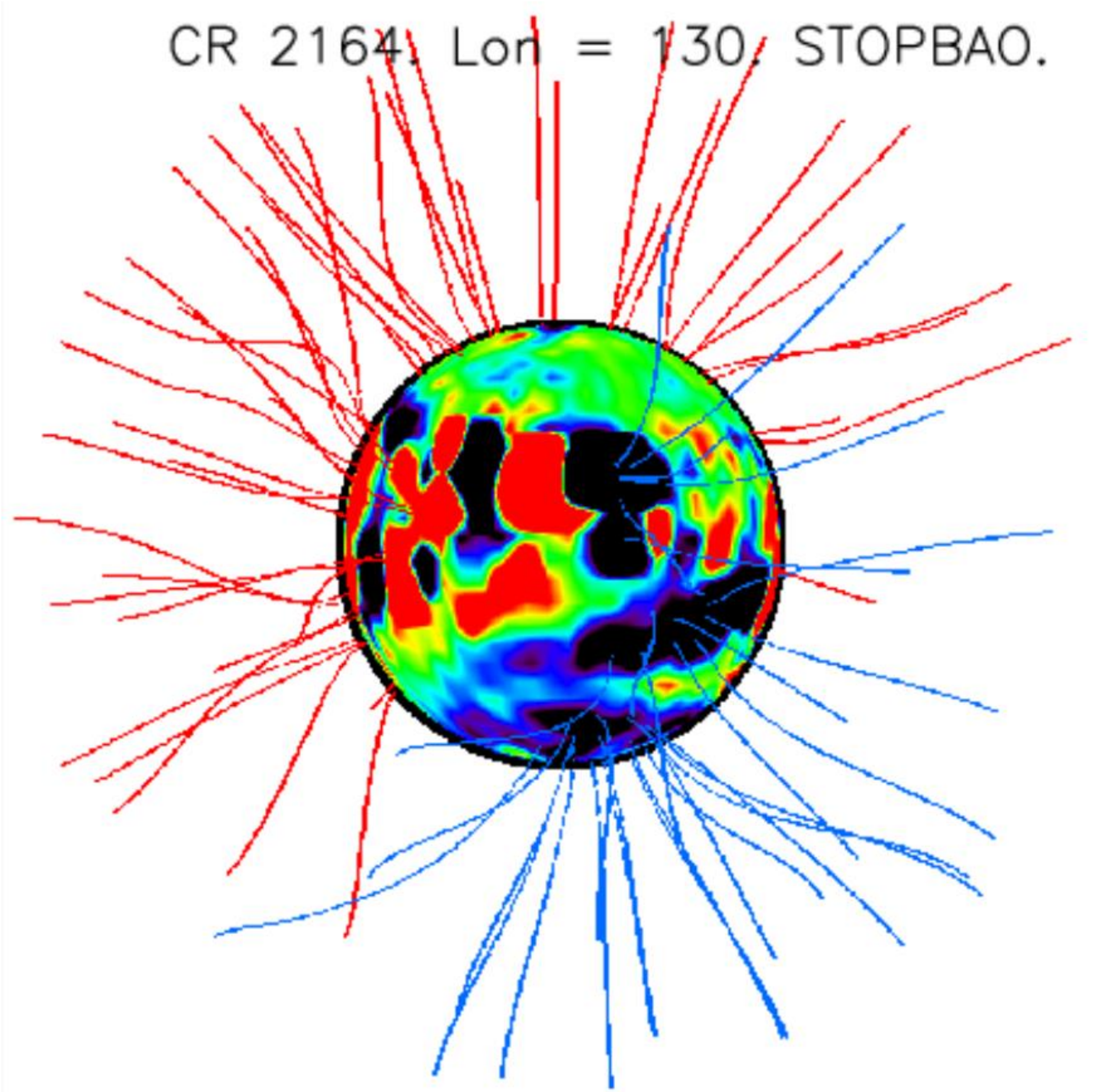
CR 2164. Lon = 130. STOPBAO.

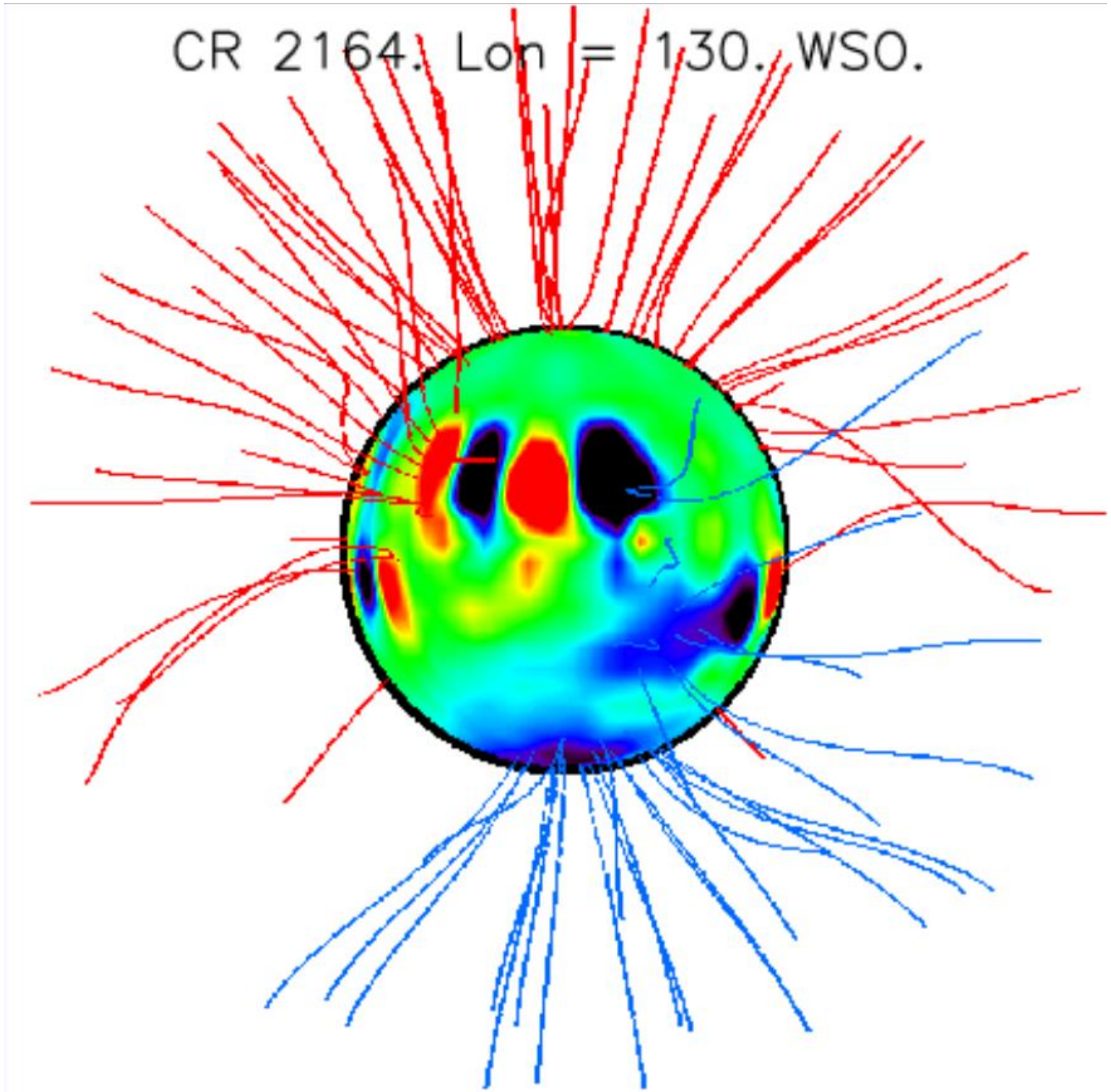
CR 2164. Lon = 130. WSO.

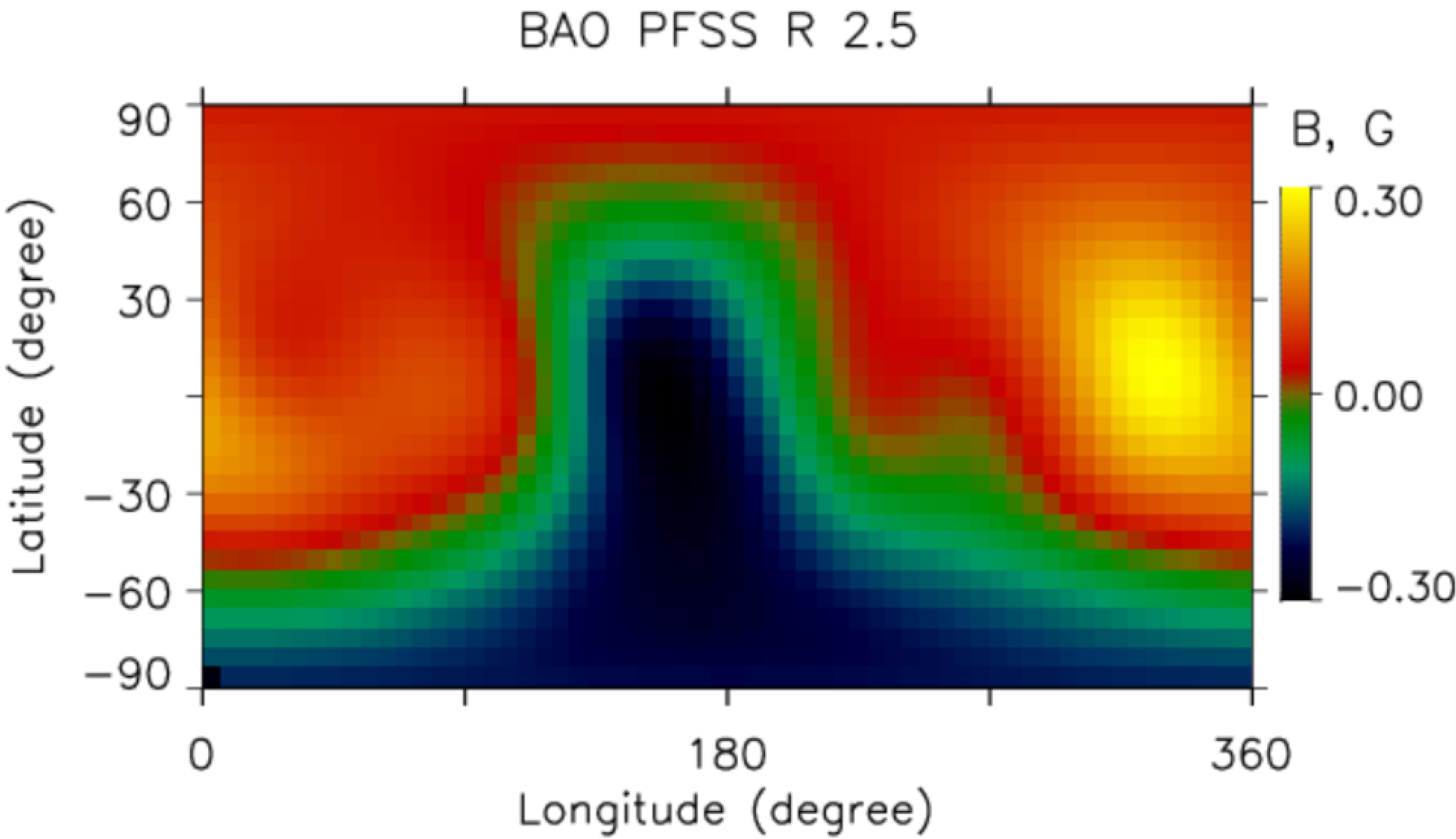
BAO PFSS R 2.5
B, G
0.30
0.00
−0.30
90
60
30
−30
−60
−90
Latitude (degree)
0
180
360
Longitude (degree)

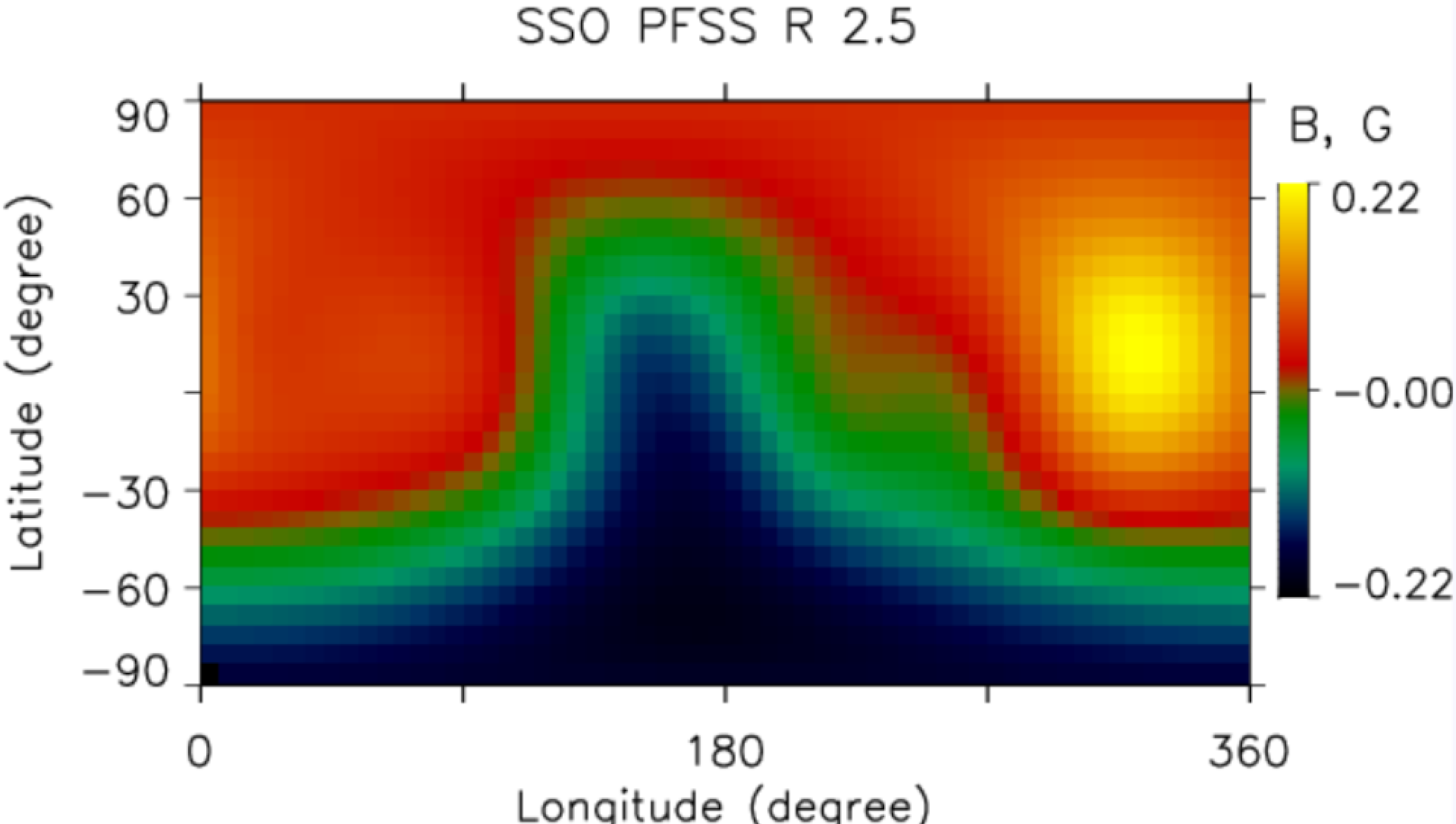
SSO PFSS R 2.5
B, G
0.22
−0.00
−0.22
90
60
30
−30
−60
−90
Latitude (degree)
0
180
360
Longitude (degree)

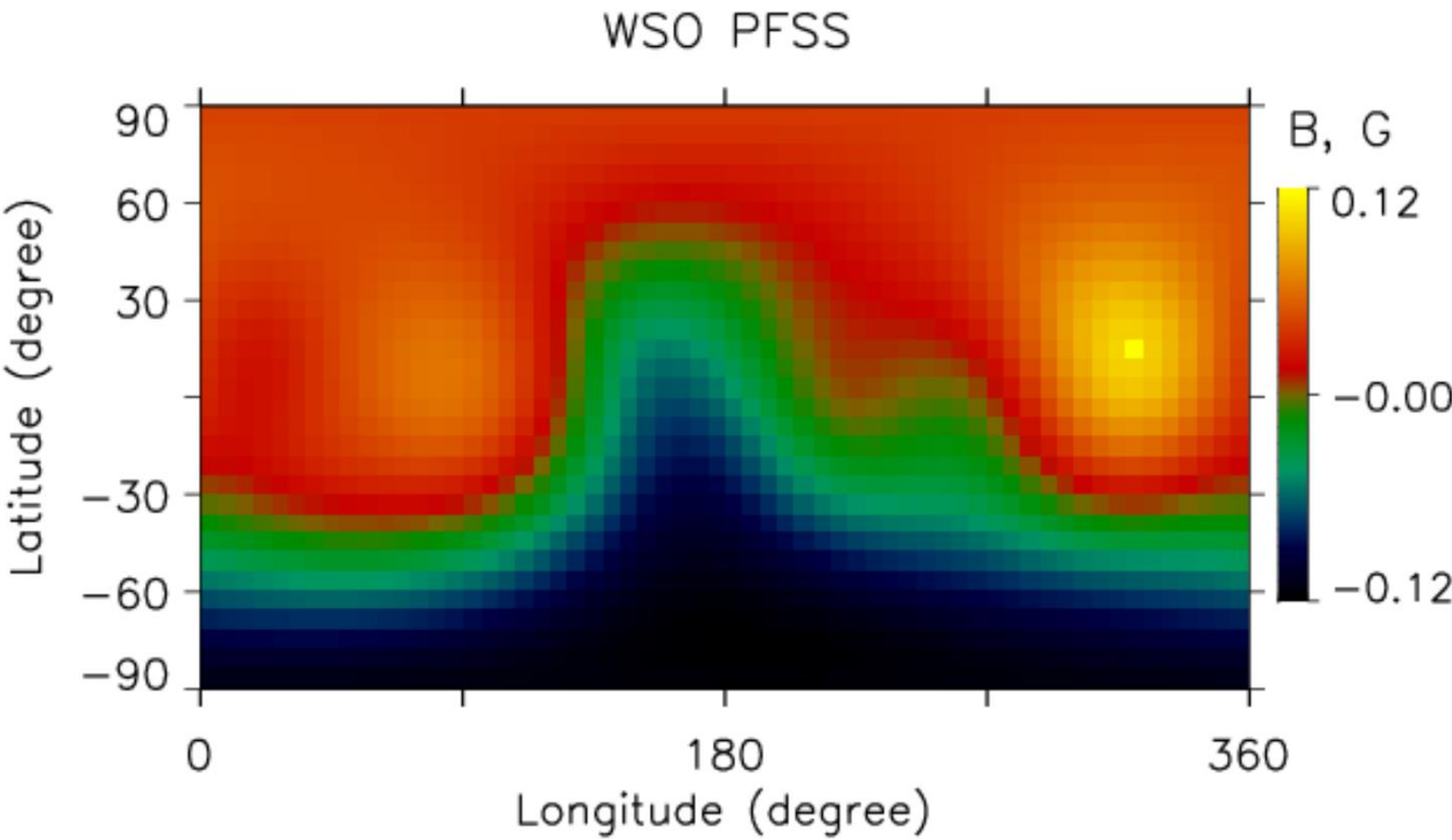

WSO PFSS
B, G
0.12
−0.00
−0.12
90
60
30
−30
−60
−90
Latitude (degree)
0
180
360
Longitude (degree)

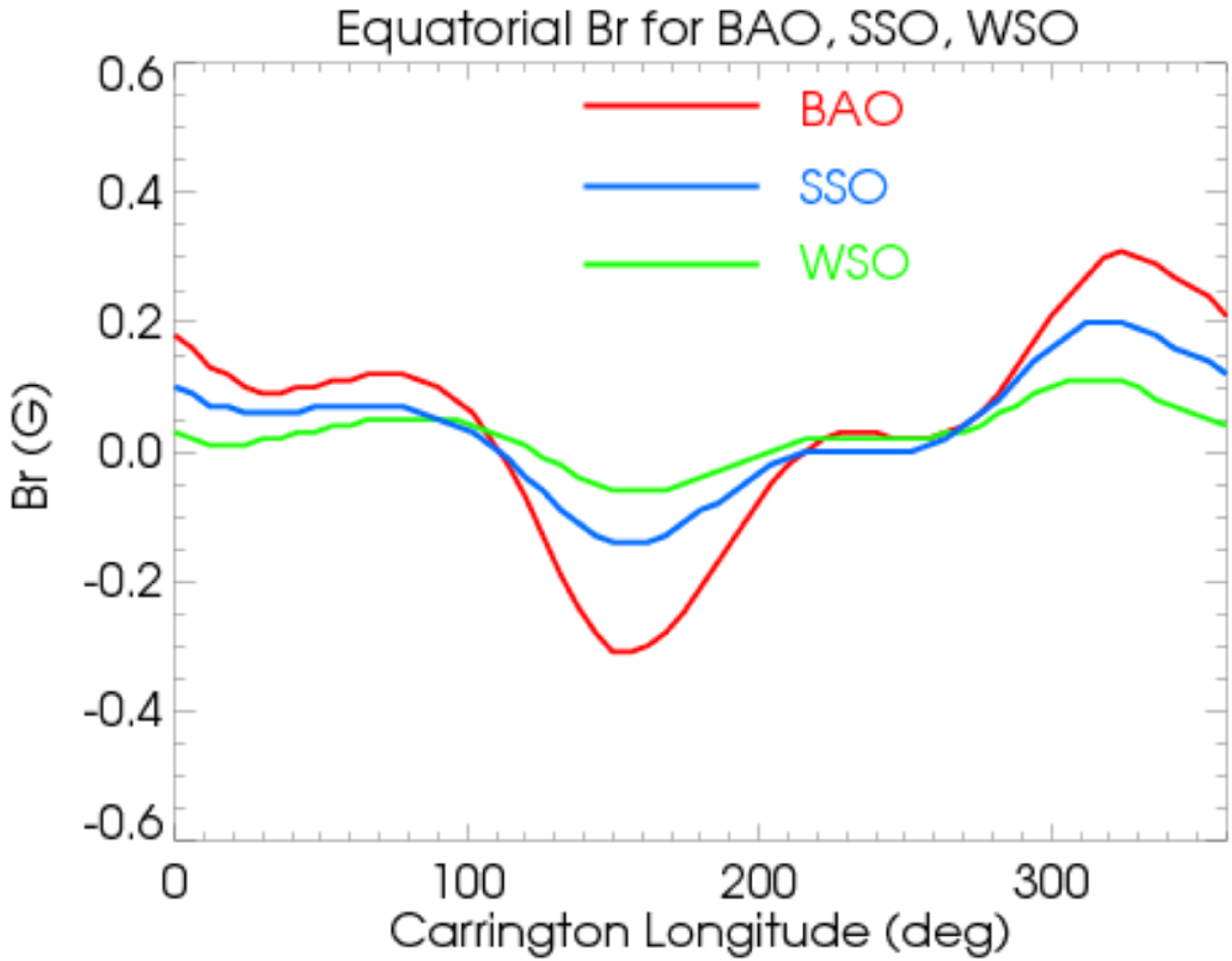

Equatorial Br for BAO, SSO, WSO
BAO
SSO
WSO
Br (G)
0.6
0.4
0.2
0.0
-0.2
-0.4
-0.6
0
100
200
300
Carrington Longitude (deg)

# WSA Basic Formula

$$V_{WSA}(f_p, d) = C_1 + C_2/(1+f_p)^{C_3} * \{C_4 - C_5 * \exp(-d/C_6)^{C_7}\}^{C_8}$$

$$f_p = (R_o/R_{ss})^2 * [B(R_o)/B(R_{ss})]$$

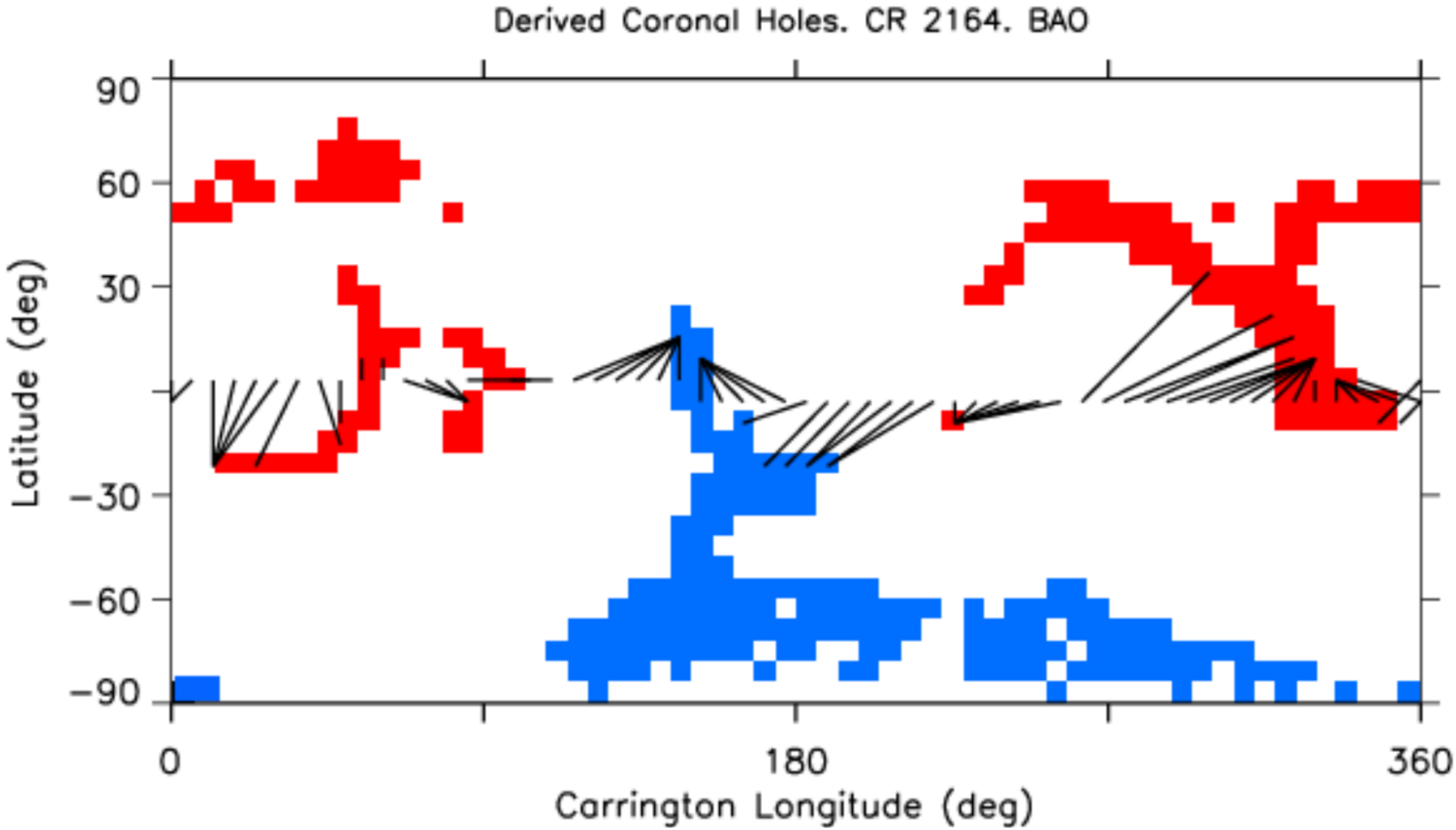

Derived Coronal Holes. CR 2164. BAO
90
60
30
−30
−60
−90
Latitude (deg)
0
180
360
Carrington Longitude (deg)

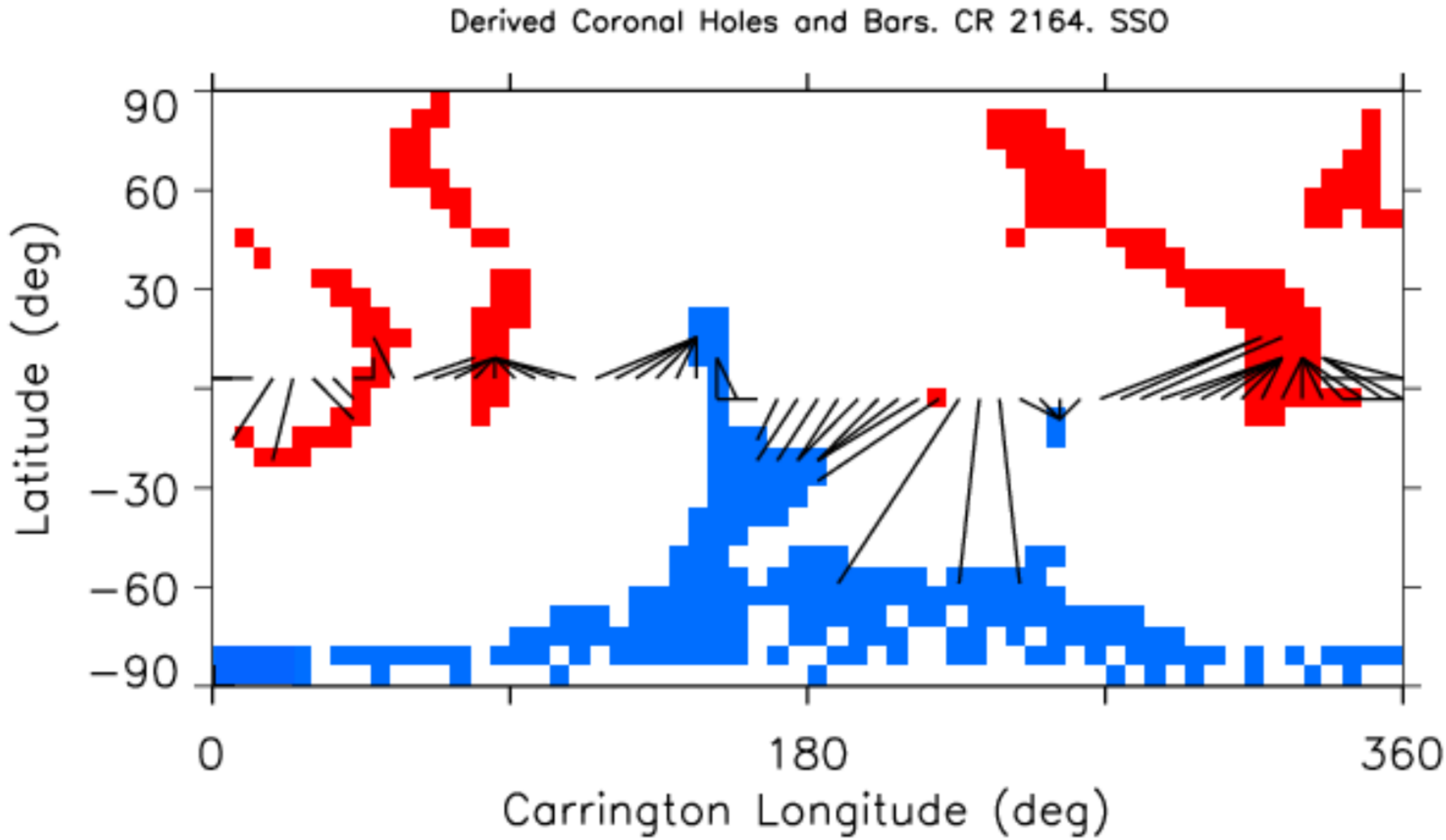

Derived Coronal Holes and Bars. CR 2164. SSO
90
60
30
-30
-60
-90
Latitude (deg)
0
180
360
Carrington Longitude (deg)

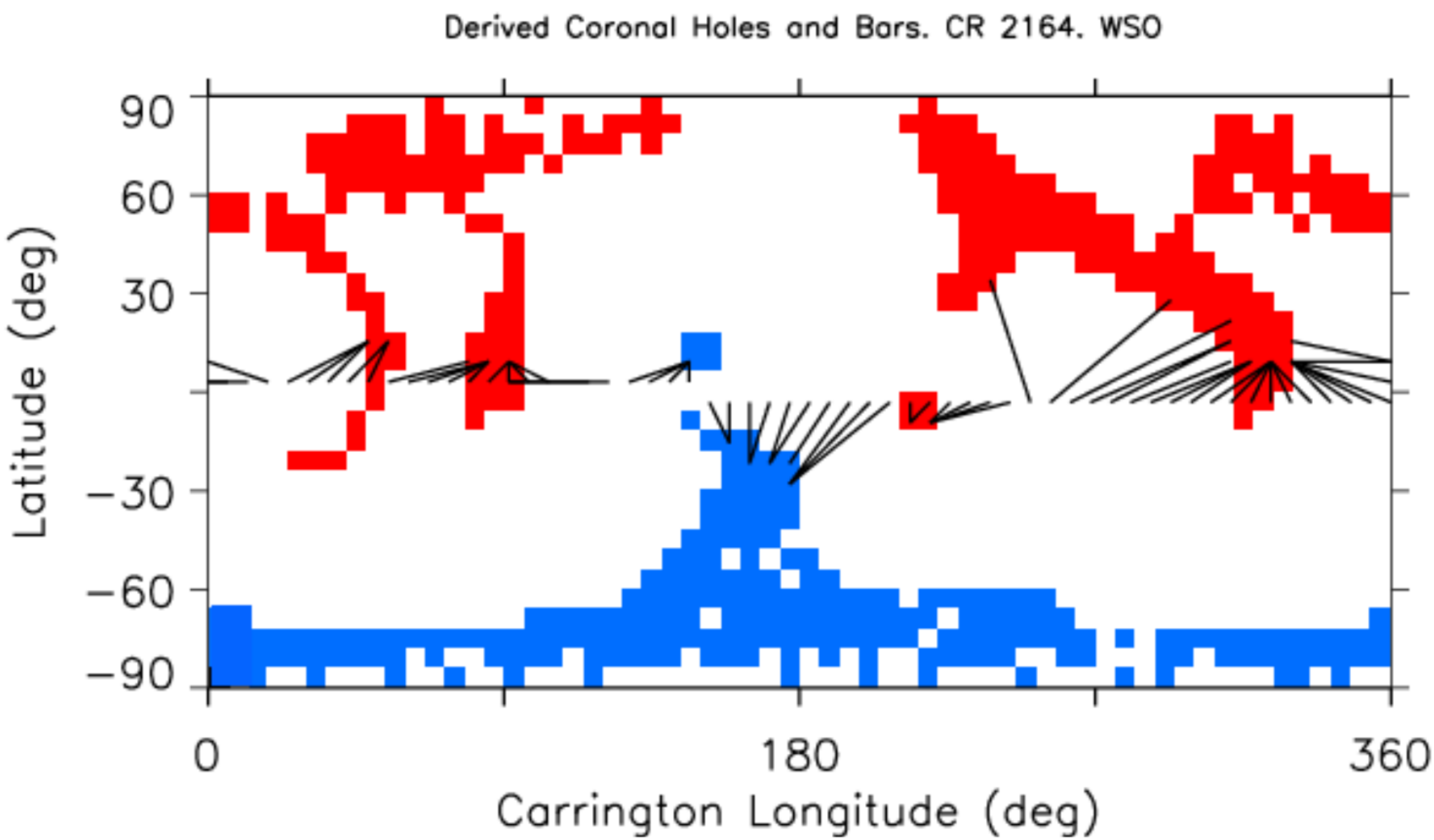

Derived Coronal Holes and Bars. CR 2164. WSO
90
60
30
−30
−60
−90
Latitude (deg)
0
180
360
Carrington Longitude (deg)

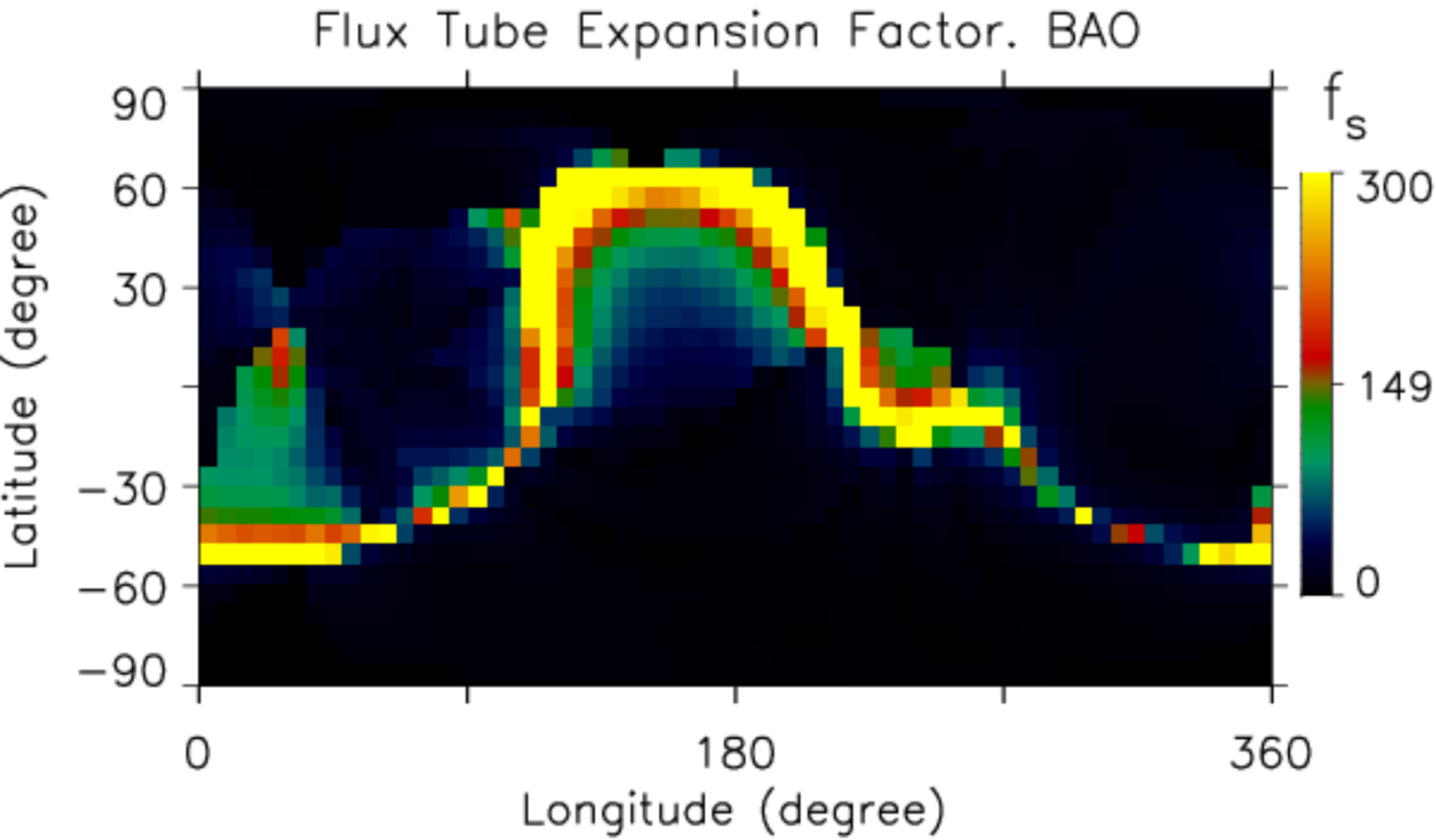
Flux Tube Expansion Factor. BAO
90
60
30
-30
-60
-90
Latitude (degree)
0
180
360
Longitude (degree)
f_s
300
149
0

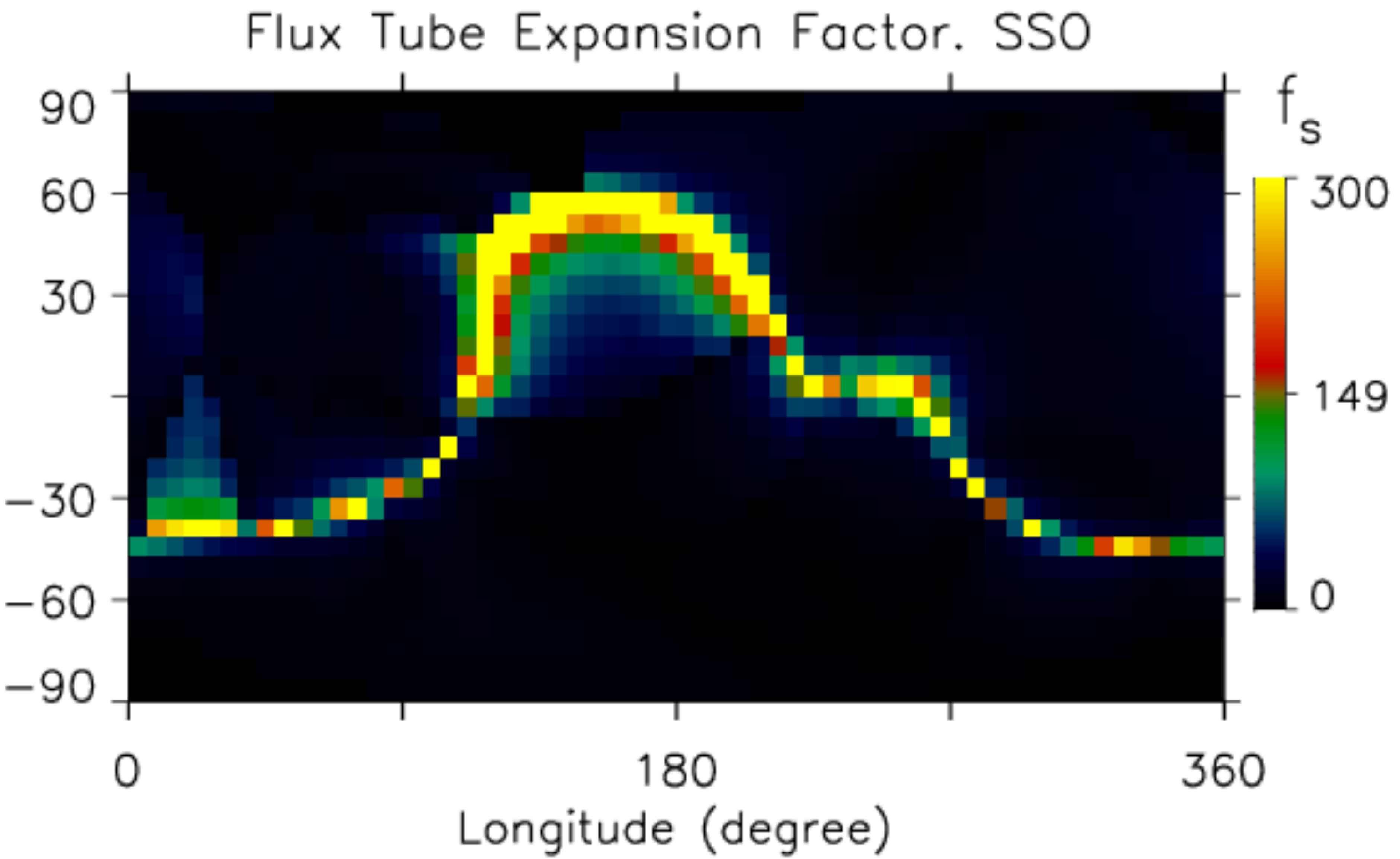
Flux Tube Expansion Factor. SSO
90
60
30
−30
−60
−90
0
180
360
Longitude (degree)
$f_s$
300
149
0

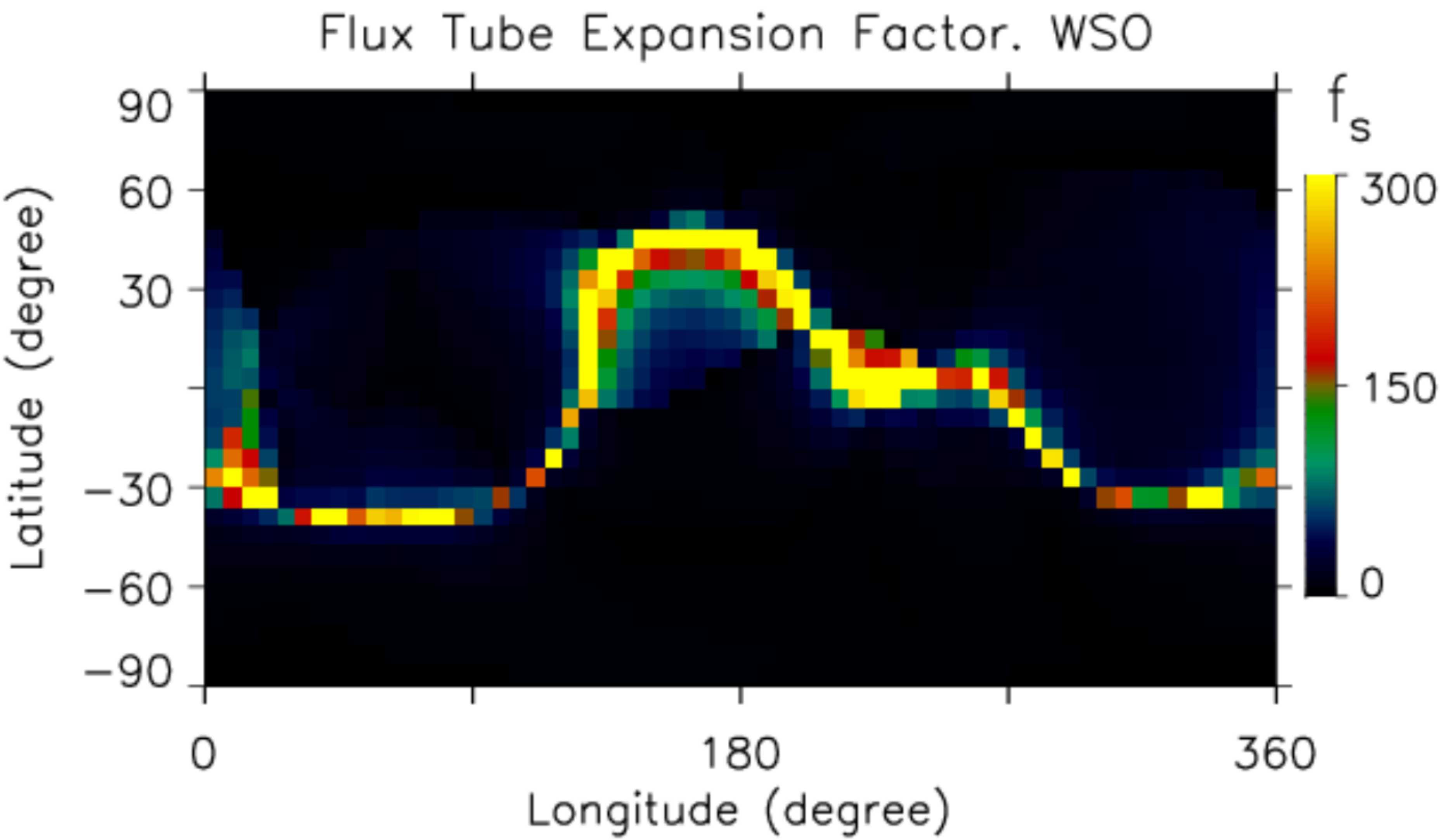
Flux Tube Expansion Factor. WSO
Latitude (degree)
90
60
30
−30
−60
−90
0
180
360
Longitude (degree)
$f_s$
300
150
0

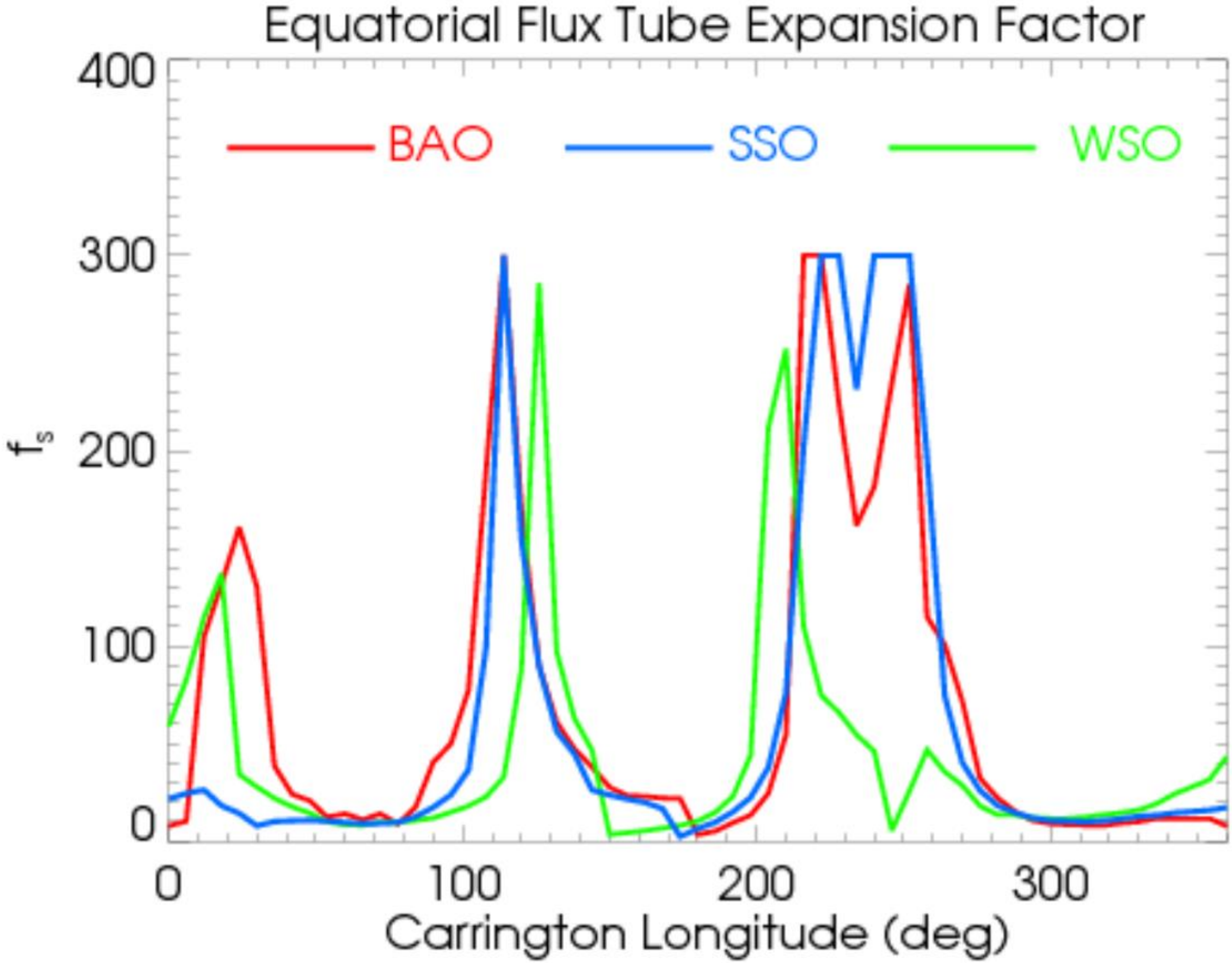

Equatorial Flux Tube Expansion Factor
BAO
SSO
WSO
$f_s$
400
300
200
100
0
0
100
200
300
Carrington Longitude (deg)

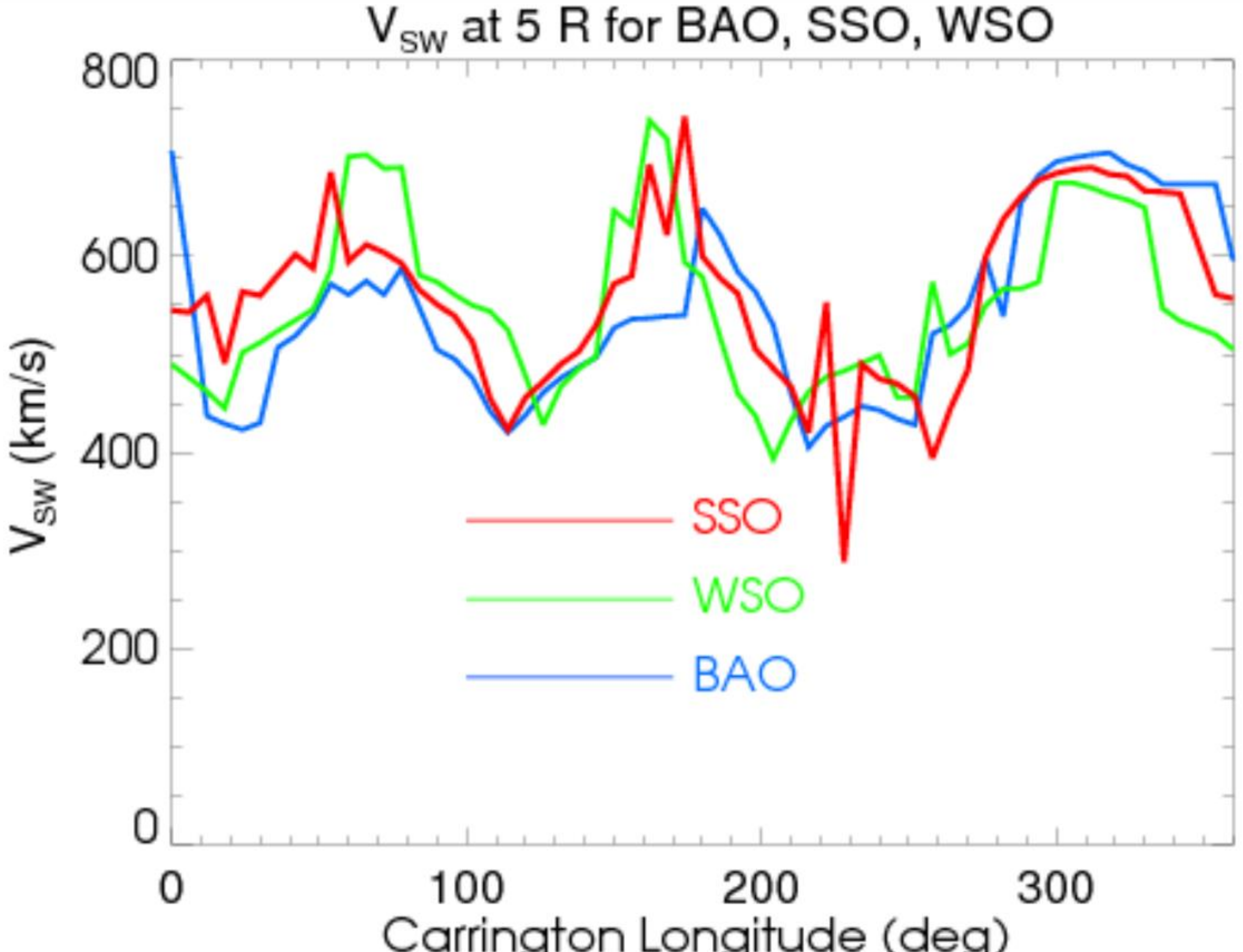

V_SW at 5 R for BAO, SSO, WSO
800
600
400
200
0
V_SW (km/s)
0
100
200
300
Carrington Longitude (deg)
SSO
WSO
BAO

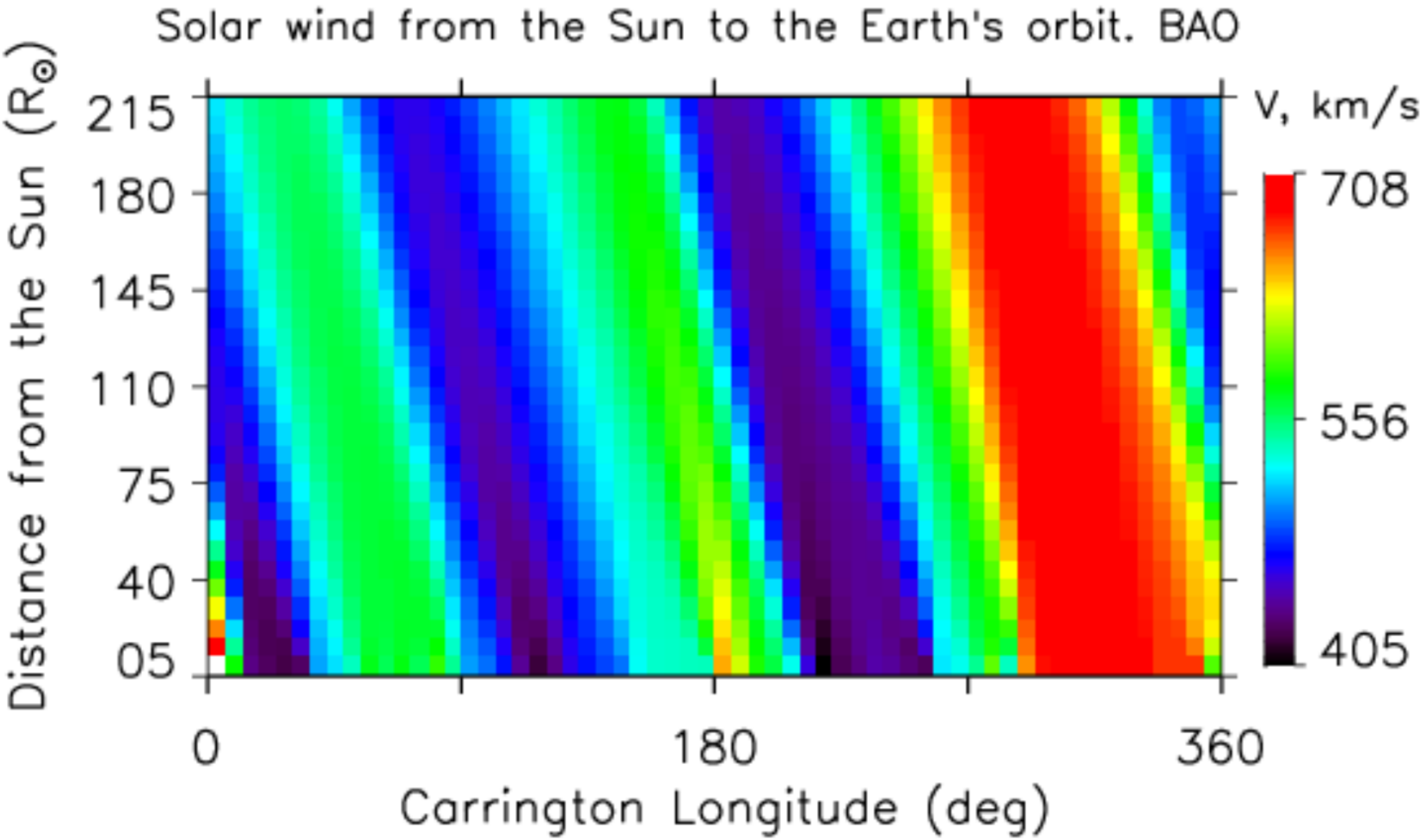
Solar wind from the Sun to the Earth's orbit. BAO
Distance from the Sun ($R_\odot$)
215
180
145
110
75
40
05
0
180
360
Carrington Longitude (deg)
V, km/s
708
556
405

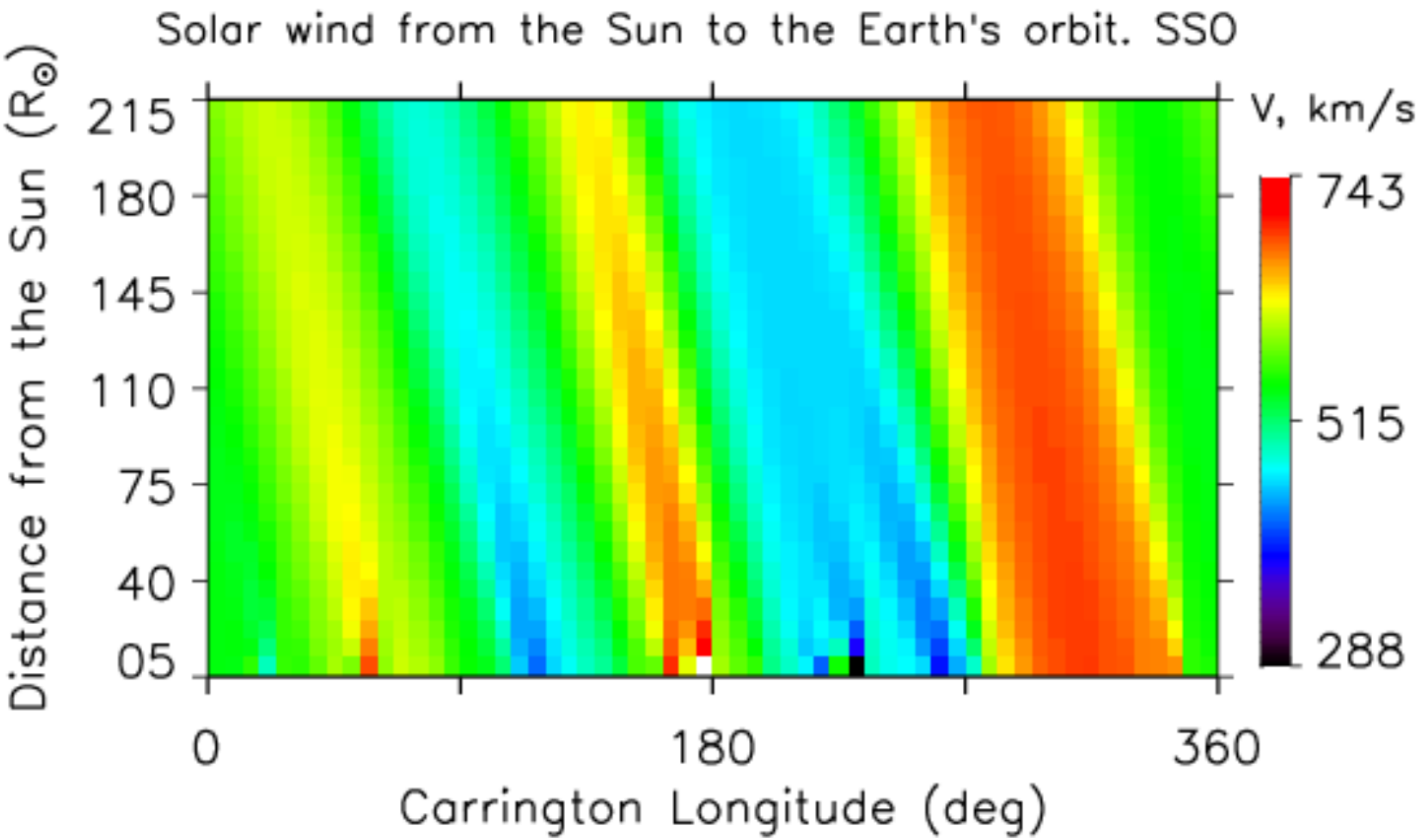
Solar wind from the Sun to the Earth's orbit. SSO
Distance from the Sun ($R_\odot$)
215
180
145
110
75
40
05
0
180
360
Carrington Longitude (deg)
V, km/s
743
515
288

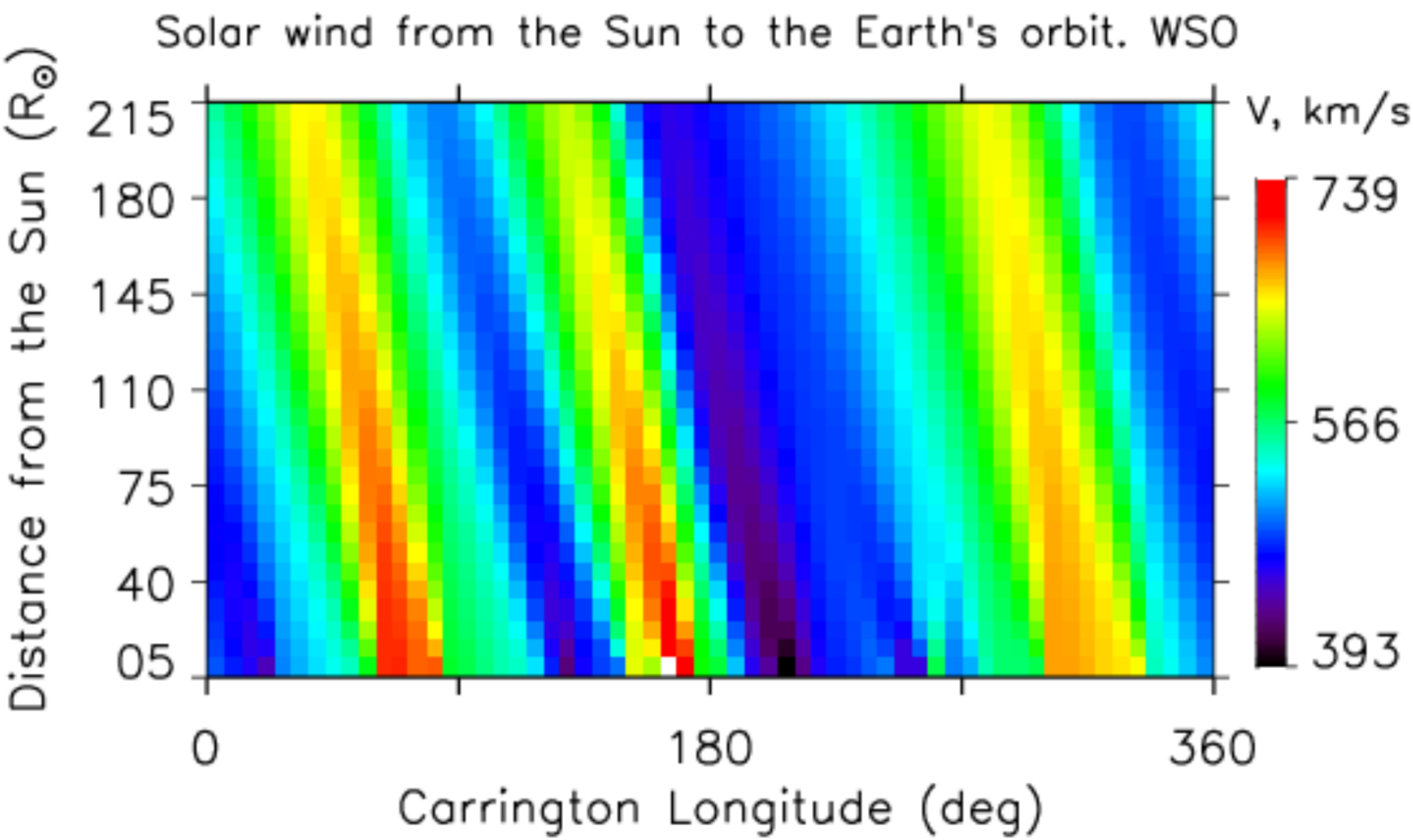
Solar wind from the Sun to the Earth's orbit. WSO
Distance from the Sun ($R_\odot$)
215
180
145
110
75
40
05
V, km/s
739
566
393
0
180
360
Carrington Longitude (deg)

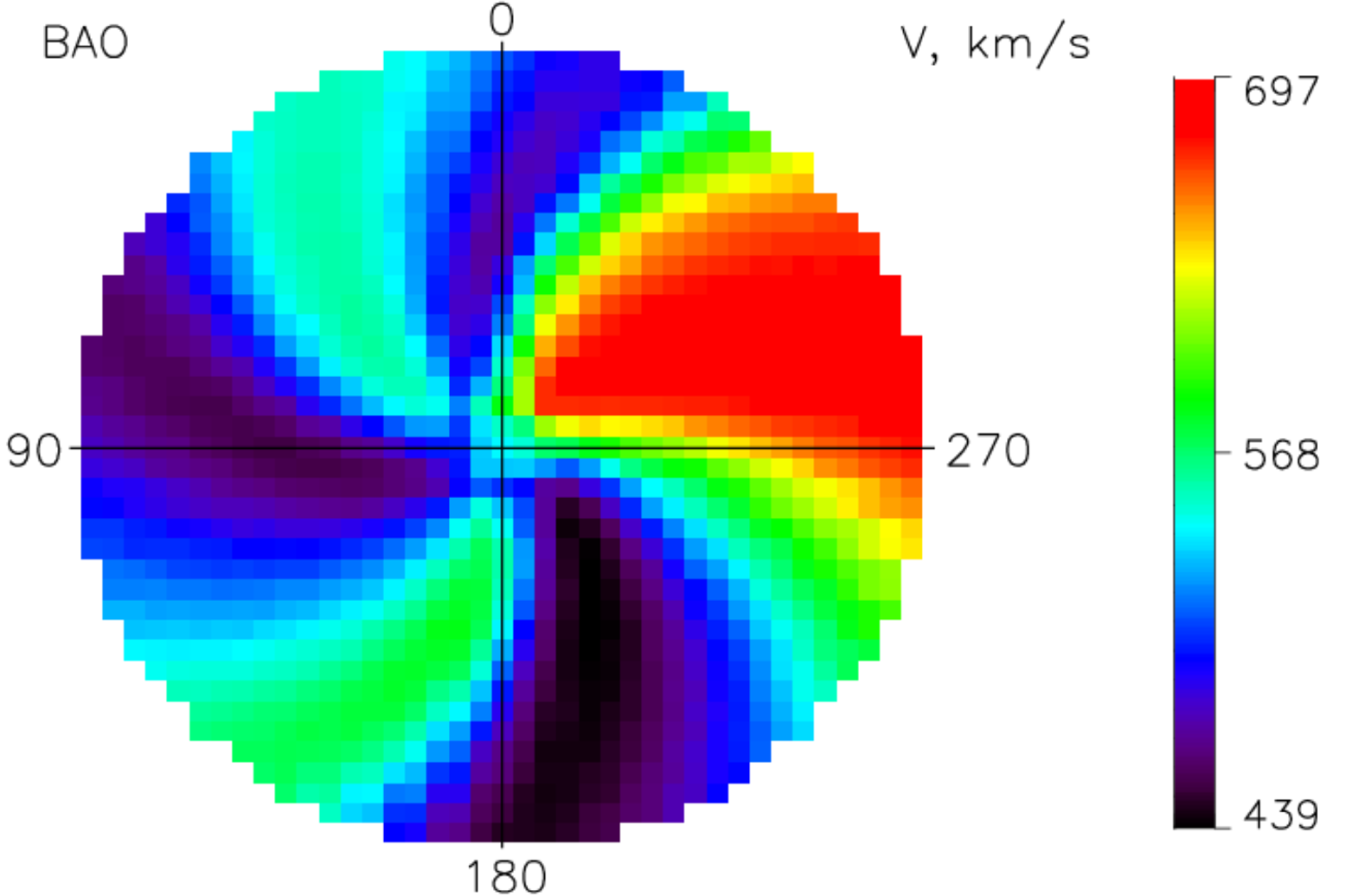
BAO
0
V, km/s
697
90
270
568
439
180

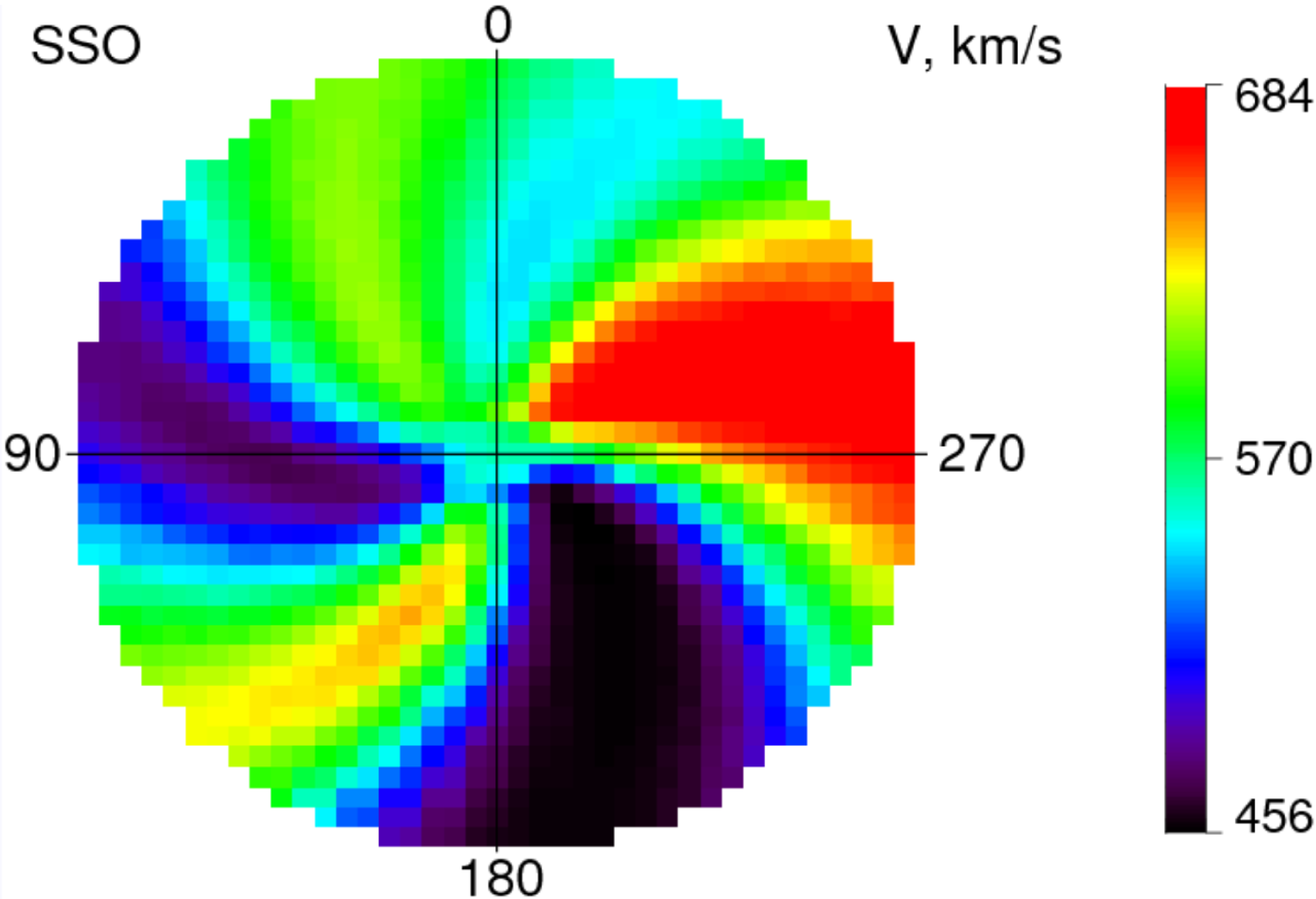
SSO
0
V, km/s
684
90
270
570
456
180

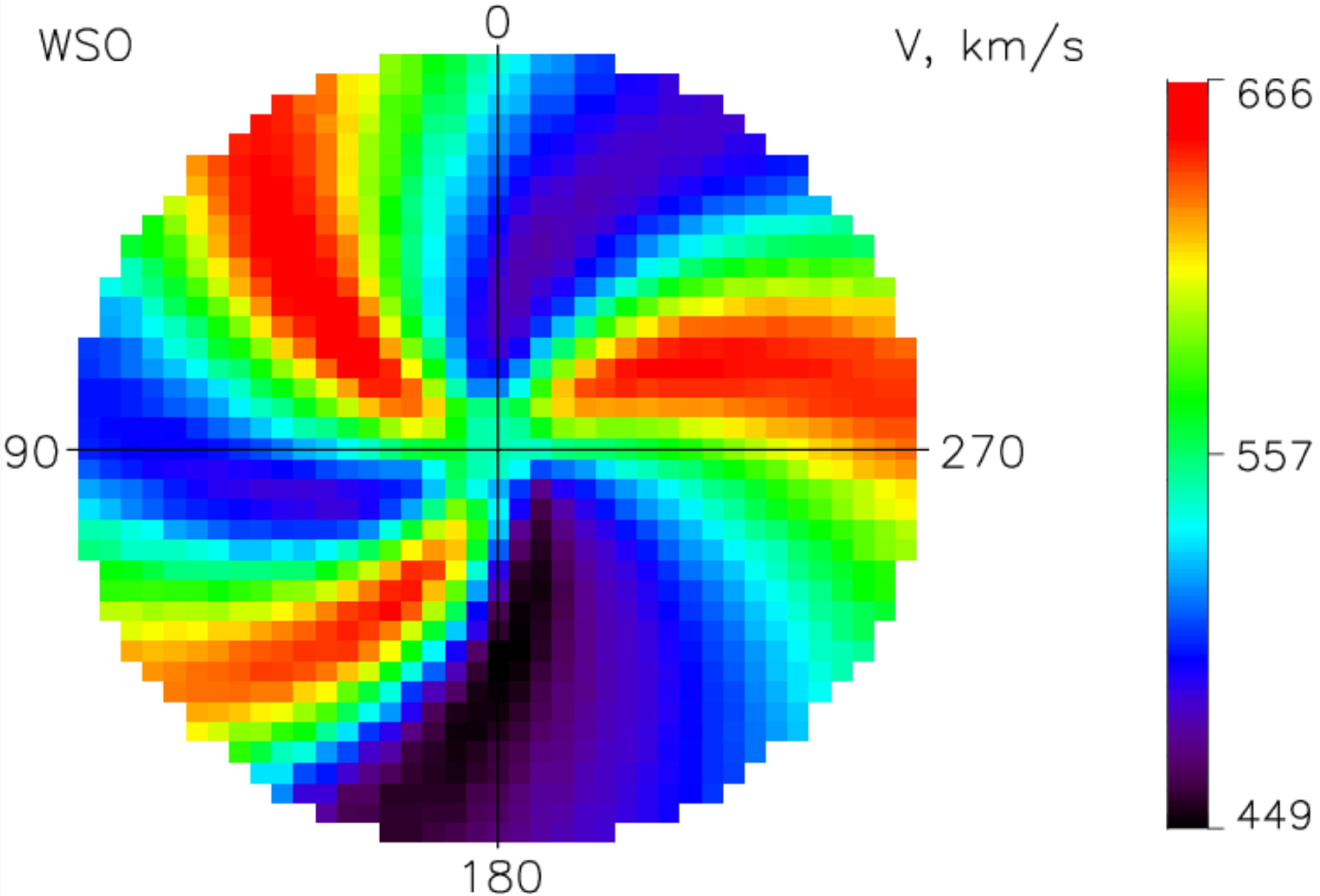
WSO
0
V, km/s
90
270
180
666
557
449

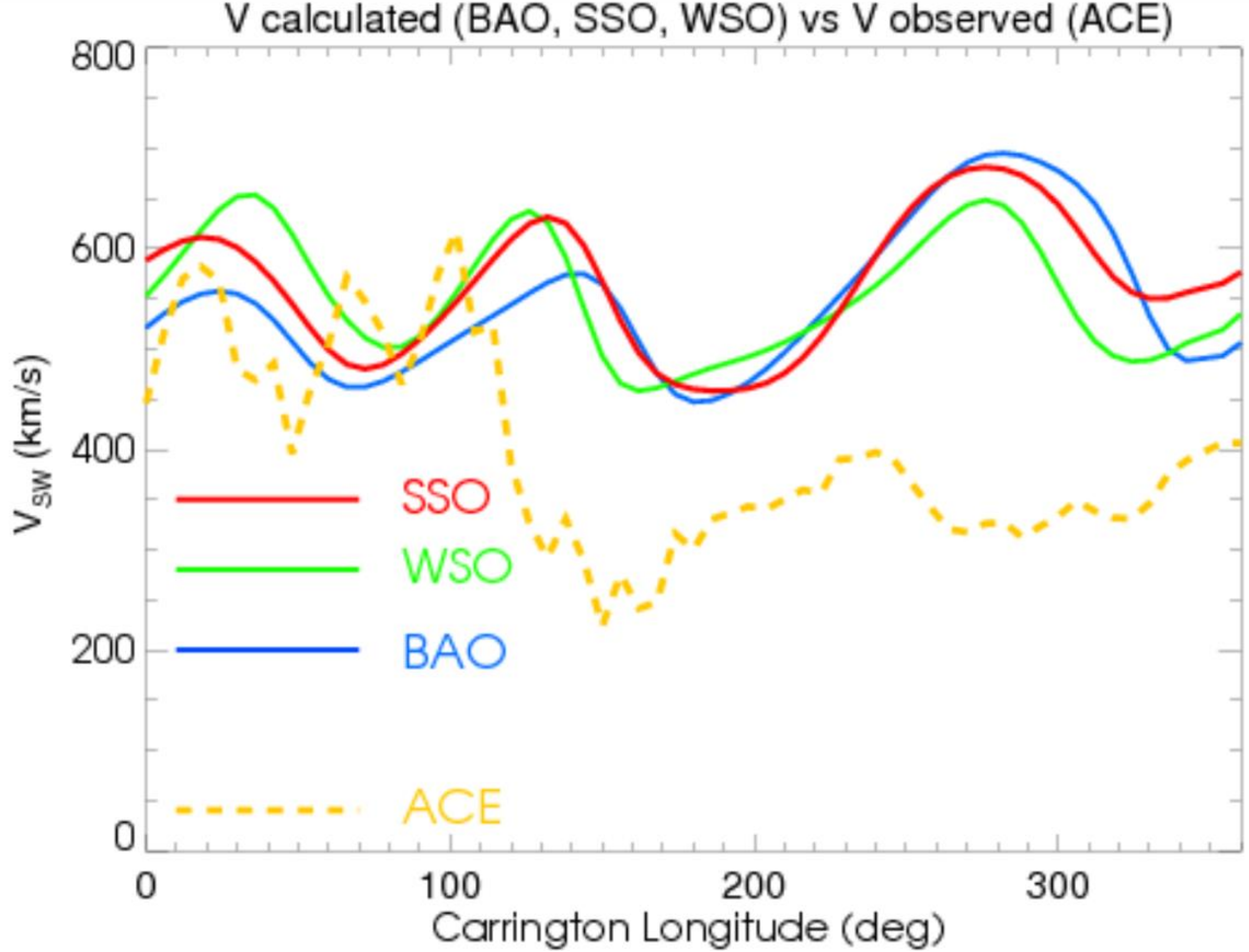

V calculated (BAO, SSO, WSO) vs V observed (ACE)
800
600
400
200
0
$V_{SW}$ (km/s)
SSO
WSO
BAO
ACE
0
100
200
300
Carrington Longitude (deg)

Баярлалаа

ᠪᠠᠶᠠᠷᠯᠠᠯᠠ ᠄

Thank you...

Спасибо...